

# Dispatching and Pricing in Two-Sided Spatial Queues

Ang Xu

Department of Industrial Engineering and Operations Research, University of California, Berkeley, angxu@berkeley.edu

Chiwei Yan

Department of Industrial Engineering and Operations Research, University of California, Berkeley, chiwei@berkeley.edu

We study a dispatching and pricing problem in two-sided spatial queues with fixed supply, motivated by ride-hailing and robotaxi platforms. Idle drivers queue on one side, waiting to pick up riders, while riders queue on the other, waiting to be matched with available drivers. The platform seeks to maximize net profit, penalized by rider waiting penalties, by jointly optimizing state-dependent dispatching and pricing decisions. We formulate this problem as a Markov decision process with state-dependent service times that capture key features of spatial matching. We show that, under mild assumptions, the optimal dispatching policy admits a closed-form expression with a *zigzag* structure. This policy significantly improves the tractability of pricing optimization due to the resulting closed-form stationary distribution and a substantially reduced state space. Building on this insight, we propose an efficient and scalable dynamic programming heuristic to approximate the optimal zigzag policy in more general settings. Extensive numerical experiments with both the analytical model and a ride-hailing simulation demonstrate that our algorithm is both near-optimal and highly scalable.

*Key words:* ride-hailing and robotaxi platforms, spatial queues, Markov decision process

*History:* First version, 07/2025.

---

## 1. Introduction

Ride-hailing services, together with the rapidly growing robotaxi industry, have revolutionized urban transportation. The dispatching process, which assigns available drivers to incoming ride requests, as well as the pricing algorithms for each incoming rider are both critical to the operational efficiency of these platforms (Yan et al. 2020). Ineffective dispatching and pricing can result in the so-called “wild goose chases” phenomenon (Castillo et al. 2025), where drivers experience long pick-up times and low utilization (the proportion of on-trip time relative to total supply minutes) due to supply shortages caused by overly aggressive dispatching (e.g., assigning drivers to riders despite long pick-up times) or insufficient price adjustments to moderate demand during peak periods.

In this paper, we study the joint dispatching and pricing problem in a two-sided spatial queueing model, where both idle drivers and riders may queue in the system while awaiting dispatch. In contrast to “one-sided” queueing models—where riders and idle drivers are matched immediately

and either the rider or driver side queues (e.g., Feng et al. 2021, Besbes et al. 2022a, Benjaafar et al. 2025)—we allow both sides to queue, and enable the platform to intentionally idle some drivers even when there are riders waiting, a strategy used often in practice when the pickup distance is long (see, e.g., Xu et al. 2020, Wang et al. 2024, Castillo et al. 2025). We briefly summarize our model.

**Model.** We develop a continuous-time Markov decision process to approximate the dispatching and pricing decisions of a ride-hailing platform with a *fixed* fleet size (e.g., robotaxi platforms). The system state tracks the number of idle drivers and waiting riders. The platform dynamically makes dispatching decisions and adjusts ride prices based on the evolving system state, aiming to maximize long-run average net profit minus rider waiting penalties. A key feature of our model is that the service rate is *state-dependent*, capturing the dynamics of spatial matching. Intuitively, as the number of idle drivers or waiting riders increases, the expected pick-up time decreases. We incorporate this dependence by modeling the service (trip completion) rate as a function of the idle driver and waiting rider counts in the system.

**Our result.** We show that, under mild assumptions on the service rate and cost coefficients, the optimal dispatching policy admits a closed-form solution (Theorem 1). Inspired by the structure of this solution, we introduce a class of dispatching policies termed *zigzag* policies. As the system state evolves, the platform’s decisions alternate between “hold” and “dispatch” in a pattern that, when visualized over the state space of drivers and riders, traces out a zigzag curve. Moreover, the zigzag policy exhibits a monotone, threshold-type structure, making it interpretable. This policy also significantly improves the tractability of pricing optimization due to the resulting closed-form stationary distribution and a substantially reduced (recurrent) state space. Building on this insight, we propose an efficient and scalable dynamic programming heuristic to approximate the optimal zigzag policy in more general settings. We evaluate our algorithm through both analytical model-based experiments and a ride-hailing simulation that captures realistic dispatching processes. In all cases, benchmarking against competitive baselines demonstrates that the zigzag policy achieves near-optimal performance and exhibits excellent scalability.

**Organization.** The remainder of the paper is organized as follows. Section 2 reviews related literature. Section 3 introduces the model, and Section 4 presents our analytical results and solution approaches. Section 5 reports extensive numerical experiments using both the analytical model and a ride-hailing simulation. We conclude in Section 6.

## 2. Literature Review

Our research is closely related to the topics of dynamic spatial matching and pricing for reusable resources, many of which are motivated by ride-hailing and shared mobility operations. We summarize the most relevant works on these two topics in the following paragraphs.

**Dynamic spatial matching.** Our work belongs to the stream of literature that use queueing-theoretic models to approximate a dynamic spatial matching system motivated from ride-hailing platforms. A prevailing modeling choice is to use state-dependent service time to capture spatial friction (e.g., Feng et al. 2021, Besbes et al. 2022a, Benjaafar et al. 2025)—the service rate of each trip increases in the number of idle drivers or the number of riders waiting in the queue, since more idle drivers or waiting riders imply a shorter pickup time, and thus, service time. Many prior studies focus on performance evaluation or capacity planning under *non-idling* dispatching policies, where idle drivers are immediately matched with waiting riders. In such settings, the queues are effectively one-sided—either on the rider or driver side, depending on availability. We consider a more general setting in which the platform is allowed to intentionally idle drivers even when riders are waiting, resulting in two-sided queues. This has connection to prior work through the use of *dispatching radius caps* (e.g., Feng et al. 2021, Wang et al. 2024, Castillo et al. 2025) or *temporal pooling* (Chen and Hu 2025), via heuristic or fluid analysis, or under “one-sided” settings (see, e.g., Xu et al. 2020 and Chen and Hu 2025). In contrast, our work aims to characterize the structure of the optimal (potentially idling) dispatching policy within a Markov decision process framework that captures two-sided queues with state-dependent service times—a formulation which is a natural extension but, to our knowledge, has not yet been addressed in the existing literature.

An important assumption of the aforementioned spatial queueing models (including our work) is that service times are independently distributed. In real dynamic spatial matching systems, however, there is often significant correlation across dispatches, as the locations of idle drivers and waiting riders tend to change little over short time intervals. Focusing on spatial correlation and non-idling dispatching policy, Kanoria (2022) considers a different framework that explicitly models the spatial locations of riders and drivers, and proposes a rate-optimal dispatching policy relative to benchmark approaches or performance bounds. On the other hand, the temporal aspect is simplified in Kanoria (2022), where all trips are assumed to be completed within a single time period. In a related spatial setting on a line, Balkanski et al. (2023) shows that a greedy policy achieves a constant competitive ratio relative to the offline optimum when each driver exits the system after serving a customer. Although our model simplifies spatial complexity through “reduced-form” Markovian queueing dynamics, we evaluate the proposed policy in a simulation environment with fully detailed spatial features and demonstrate its effectiveness.

**Pricing in (spatial) service systems.** The pricing aspect of our work also relates to the literature on pricing in (spatial) service systems. Conceptually speaking, our work is closely related to Castillo et al. (2025), which demonstrates the need for surge pricing to avoid “wild goose chases” and ensure low pick-up times, thereby restoring the demand-supply balance. Methodologically, our work is most relevant to Banerjee et al. (2015), Besbes et al. (2022b), Bergquist and Elmachtoub (2024), and Elmachtoub and Shi (2025), which study pricing for reusable resources modeled using Markovian queueing dynamics. Many of these studies focus on analyzing the performance of static pricing policies. A distinguishing feature of our work is the incorporation of state-dependent service rates, in contrast to prior studies that assume a fixed service rate, rendering many of their insights not directly applicable. State-dependent service rates also make the service policy non-trivial, making the pricing policy tightly coupled with the complexity of the service policy. One implication of our proposed zigzag dispatching policy is that the induced Markov chain effectively reduces to a birth-death process with a state space that is an order of magnitude smaller than the original. This structure also admits a closed-form (product-form) stationary distribution, making the pricing optimization problem more tractable.

### 3. Model and Preliminaries

We consider a ride-hailing or robotaxi platform operating a fixed fleet to serve riders across a service region. Rider arrivals into the service region follow a Poisson process with rate  $\Lambda$ . Upon arrival, each rider is quoted a price that may depend on the current system state. If a rider accepts the price, she joins a queue to await matching with a driver. The platform can decline to serve a rider by setting the price at or above a certain threshold. Importantly, the platform is not required to dispatch a driver immediately when a rider agrees to the price; it may delay dispatch even when idle drivers are available. We assume riders are patient—once they join the queue, they will wait until matched with an idle driver. However, the platform incurs a penalty for rider waiting times in its objective, and thus seeks pricing and dispatching policies that maximize net profit minus rider waiting penalties, as detailed later.

#### 3.1. State, Action, and Policy

Let  $L$  denote the total number of drivers in the system, and let  $\mathcal{L} := \{0, 1, \dots, L\}$  be the index set of possible driver counts. The state space is defined as  $\mathcal{S} := \{(l, m) : l \in \mathcal{L}, m \in \mathbb{Z}_{\geq 0}\}$ , where each state  $(l, m)$  represents  $l$  drivers currently *in service* and  $m$  riders *waiting in the queue*. State transitions occur due to three types of events: (1) *Trip completion*: when a driver completes a trip, he immediately becomes idle and the state transitions from  $(l, m)$  to  $(l + 1, m)$ ; (2) *Rider arrival*: when a new rider arrives and accepts the price to join the queue, the state transitions from  $(l, m)$

to  $(l, m + 1)$ ; (3) *Dispatching decision*: when the platform dispatches  $k$  drivers to pick up  $k$  waiting riders (with  $k \leq m$ ), the state transitions from  $(l, m)$  to  $(l + k, m - k)$ . The platform may dispatch multiple drivers simultaneously at any decision epoch. For example, if the system is in state  $(l, m)$ , a trip is then completed, and the platform decides to immediately dispatch two drivers to pick up two riders, the state transitions to  $(l - 1 + 2, m - 2) = (l + 1, m - 2)$ .

The platform's actions consist of two components: *pricing* and *dispatching*. At each state transition, the platform updates both the price for incoming riders and its dispatching decisions. We assume the trip price is given by  $p = p_0 + p_1 d$ , with  $p_0 \geq 0$  denoting a fixed base fare, and  $p_1 \in [0, p_{\max}]$  representing the per-kilometer charge that can be dynamically adjusted by the platform (e.g., via surge pricing). Riders' willingness to pay per kilometer is drawn from a cumulative distribution function (CDF)  $F(\cdot)$ . A rider will accept the price and join the queue if and only if their willingness to pay per kilometer exceeds or equals  $p_1$ . Thus, the *effective request rate* (or request conversion rate) is  $\lambda = \Lambda \bar{F}(p_1)$ ,<sup>1</sup> where  $\bar{F}(p_1) = 1 - F(p_1)$  denotes the tail CDF of riders' willingness to pay. We assume a one-to-one correspondence between  $\lambda$  and  $p_1$ , with  $\bar{F}(0) = 1$ ,  $\bar{F}(p_{\max}) = 0$ , and  $\bar{F}(p_1)$  strictly decreasing in  $p_1$ . Therefore, setting  $p_1$  is equivalent to setting  $\lambda$ , and we denote by  $p_1(\lambda)$  the per-kilometer price corresponding to an effective request rate  $\lambda$ . For notational convenience, we define the *pricing policy* as a mapping  $\lambda : \mathcal{S} \rightarrow [0, \Lambda]$ , where  $\lambda(l, m)$  specifies the effective request rate at state  $(l, m)$ . In the following, we describe pricing decisions in terms of  $\lambda$  rather than  $p$ .

A *dispatching policy*  $\phi : \mathcal{S} \mapsto \{0, 1\}$  maps the state space to a binary number, which determines whether the platform dispatches available drivers to riders at state  $(l, m)$ . In specific,  $\phi(l, m) = 1$  represents the dispatching action, and  $\phi(l, m) = 0$  the holding action (no dispatching) under state  $(l, m)$ . The system transitions from state  $(l, m)$  to state  $(l + 1, m - 1)$  if  $\phi(l, m) = 1$ . At the new state  $(l + 1, m - 1)$ , the platform considers again whether to dispatch and repeats this process until policy  $\phi$  at the current state indicates a holding action. For example, suppose the dispatching policy  $\phi$  is defined as  $\phi(1, 3) = \phi(2, 2) = 1$  and  $\phi(3, 1) = 0$ . If a new rider arrives when the system is in state  $(l, m) = (1, 2)$ , the state first changes to  $(1, 3)$ . Since  $\phi(1, 3) = 1$ , a driver is dispatched, causing the state to transition to  $(2, 2)$ . Similarly, because  $\phi(2, 2) = 1$ , another driver is dispatched, and the state transitions to  $(3, 1)$ . Note that the platform is able to dispatch only when there is at least one idle driver and one rider in the queue. Thus, for any policy, we have  $\phi(l, 0) = 0$  for all  $l \in \mathcal{L}$  and  $\phi(L, m) = 0$  for all  $m \in \mathbb{Z}_{\geq 0}$ . Note that the system will never remain in a state  $(l, m)$  with  $\phi(l, m) = 1$ , as all dispatching actions are executed instantaneously without delay.

<sup>1</sup> The dependence of demand on  $p_0$  is captured by the exogenous arrival rate  $\Lambda$ , as the model does not permit  $p_0$  to be altered.

### 3.2. Service (Trip Completion) Rate

For each trip, the service time consists of two parts: “pick-up time” and “on-trip time”. Pick-up time is the duration it takes for the driver to travel from his current location to the rider’s arrival location. On-trip time is the duration for the driver to travel from the rider’s arrival location to her desired destination. Instead of modeling the real-time locations of riders and drivers, following related literature such as Feng et al. (2021), Besbes et al. (2022a) and Benjaafar et al. (2025), we adopt a “reduced-form” setting which approximates the service time of each driver in service at state  $(l, m)$  as an exponential<sup>2</sup> random variable with rate  $\mu_{l,m}$  which increases with  $m$  and decreases with  $l$ .<sup>3</sup> Intuitively, as the number of idle drivers or waiting riders increases, the expected pick-up time decreases. For example, if the platform matches the closest idle driver and rider pair when making a dispatch decision—a common practice in the industry (Yan et al. 2020)—a larger pool of waiting drivers or riders enables better matches. We also assume that there exists a  $\bar{\mu} > 0$  such that  $\mu_{l,m} \leq \bar{\mu}$  for all  $(l, m) \in \mathcal{S}$ . The boundedness assumption for  $\mu_{l,m}$  is motivated by the fact that the service time necessarily includes a non-negligible on-trip component. The trip completion rate at state  $(l, m)$  is thus  $l\mu_{l,m}$ .

### 3.3. Objective

Our objective balances two components: (1) improving the platform’s expected long-run average profit (i.e., revenue minus operating costs), and (2) reducing penalties associated with rider queuing and pickup delays.

**Platform revenue.** Let  $\mathcal{R}(\lambda, \phi, T)$  be the cumulative revenue up to time  $T$  under policy  $(\lambda, \phi)$ . We denote the corresponding long-term average revenue rate by  $\mathcal{R}(\lambda, \phi) := \lim_{T \rightarrow \infty} \mathbb{E}[\mathcal{R}(\lambda, \phi, T)]/T$ . Note that some policies may lead to unstable queues, where the number of riders in the queue grows indefinitely. However, without loss of optimality, we can restrict our analysis to policies that ensure queue stability, as unstable policy leads to infinitely large rider waiting penalties, as we will introduce next. When the queue is stable, the stationary distribution exists for each state as the underlying unichain is ergodic. Let  $\pi_{\lambda, \phi}(l, m)$  be the stationary distribution of having  $l$  drivers in service and  $m$  riders in the queue under policy  $(\lambda, \phi)$ . Suppose that the on-trip time for each ride has a mean  $t_0$ , and the driving speed of all vehicles is 1. Then we can write  $\mathcal{R}(\lambda, \phi)$  as

$$\mathcal{R}(\lambda, \phi) = \sum_{(l,m) \in \mathcal{S}} \pi_{l,m}(\lambda, \phi) \lambda(l, m) (p_0 + p_1(\lambda(l, m)) \cdot t_0). \quad (1)$$

<sup>2</sup> In real world, service times may be correlated with past history of arrivals and dispatches. For tractability, we ignore this dependence and assume that service times are independent and memoryless.

<sup>3</sup> In fact, the monotonicity of  $\mu_{l,m}$  is *not* required in our analysis, although it is well expected in real-world spatial systems.

**Operating cost and rider waiting penalties.** We consider the following quantities under policy  $(\lambda, \phi)$ : (1) the expected number of drivers in service (including those en route to pick-ups and on trips), denoted by  $L_s^d(\lambda, \phi)$ ; (2) the expected number of idle (available) drivers, denoted by  $L_o^d(\lambda, \phi)$ , where  $L_o^d(\lambda, \phi) = L - L_s^d(\lambda, \phi)$ ; (3) the expected number of riders waiting to be picked up, denoted by  $L_p^r(\lambda, \phi)$ ; and (4) the expected number of riders in the queue awaiting a match, denoted by  $L_q^r(\lambda, \phi)$ . Our objective can be expressed as

$$\sup_{\lambda, \phi} \underbrace{\mathcal{R}(\lambda, \phi)}_{\text{revenue rate}} - \underbrace{w_s^d L_s^d(\lambda, \phi) - w_o^d L_o^d(\lambda, \phi)}_{\text{driving/operating cost rate}} - \underbrace{w_p^r L_p^r(\lambda, \phi) - w_q^r L_q^r(\lambda, \phi)}_{\text{penalty rate from rider waiting}}, \quad (2)$$

where  $w_s^d, w_o^d, w_p^r$  and  $w_q^r$  are positive constants measuring cost/penalties per unit time and driver/rider. In particular,  $L_s^d(\lambda, \phi)$  and  $L_o^d(\lambda, \phi)$  denote the operating costs for drivers while in service and while idle, respectively, with  $w_s^d \geq w_o^d$  typically holding since idle drivers generally consume less fuel or electricity. Similarly,  $L_p^r(\lambda, \phi)$  and  $L_q^r(\lambda, \phi)$  capture the penalties associated with riders waiting in the queue and those waiting to be picked up, respectively. Usually,  $w_p^r \geq w_q^r$ , as riders are generally more sensitive to waiting in the queue than after a driver has been dispatched to them. Calculating the objective in (2) directly can be challenging, as the expected number of riders waiting to be picked up,  $L_p^r(\lambda, \phi)$ , cannot be explicitly determined from the system state. Fortunately, an equivalent and much simpler form of the objective function can be derived. Let  $\mathcal{R}(\lambda, \phi; p_0)$  denote the value of  $\mathcal{R}(\lambda, \phi)$  for a given  $p_0$ .

LEMMA 1. *We have  $\arg \max_{\lambda, \phi} \mathcal{R}(\lambda, \phi; p_0) - w_s^d L_s^d(\lambda, \phi) - w_o^d L_o^d(\lambda, \phi) - w_p^r L_p^r(\lambda, \phi) - w_q^r L_q^r(\lambda, \phi) = \arg \max_{\lambda, \phi} \mathcal{R}(\lambda, \phi; p_0 + w_p^r t_0) - (w_s^d + w_p^r - w_o^d) L_s^d(\lambda, \phi) - w_q^r L_q^r(\lambda, \phi)$ .*

Lemma 1 shows that, by appropriately resetting the value of  $p_0$  and the cost/penalty coefficients, both  $L_o^d(\lambda, \phi)$  and  $L_p^r(\lambda, \phi)$  can be omitted from the objective, while the optimal policy remains unchanged. To see the intuition, since drivers are either in service or idle, in (2), the driving/operating cost rate can be rewritten as the following two parts: (i) a penalty term  $w_o^d L$  that accrues for all drivers and (ii) a penalty term  $(w_s^d - w_o^d) L_s^d(\lambda, \phi)$  that accrues only for drivers who are in service. Without loss of optimality, we can ignore the penalty term in part (i), as it is independent of  $\lambda$  and  $\phi$ . Thus,  $L_o^d(\lambda, \phi)$  can be omitted from our objective. Likewise, when a driver is in service, she is either picking up a rider or on a trip to the destination. Therefore, we can rewrite  $L_p^r(\lambda, \phi)$  as  $L_s^d(\lambda, \phi)$  minus the average number of on-trip drivers. One can show that the on-trip component is equivalent to increasing  $p_0$  by  $w_p^r t_0$ . This allows us to omit  $L_p^r(\lambda, \phi)$  as well. In the resulting optimization problem, the expected number of drivers in service  $L_s^d(\lambda, \phi)$  and the expected number of riders in the queue  $L_q^r(\lambda, \phi)$  can be directly calculated from the states  $(l, m)$

and the corresponding stationary distribution. For conciseness, in the remainder of the paper, we set driver-side penalty  $c_d := w_s^d + w_p^r - w_o^d$  and rider-side penalty  $c_r := w_r^r$ . Our new (equivalent) objective, denoted by  $\tilde{\mathcal{R}}(\lambda, \phi)$ , becomes

$$\sup_{\lambda, \phi} \tilde{\mathcal{R}}(\lambda, \phi) := \sup_{\lambda, \phi} \sum_{(l, m) \in \mathcal{S}} \pi_{\lambda, \phi}(l, m) (\lambda(l, m) (p_0 + w_p^r t_0 + p_1(\lambda(l, m)) \cdot t_0) - c_d l - c_r m). \quad (3)$$

Our goal is to develop efficient solution approaches to find an optimal policy  $(\lambda^*, \phi^*)$  that maximizes this objective, as we will discuss next.

## 4. Solution Approaches

The system described in Section 3 is a *continuous-time Markov decision process* (CTMDP) with a countably infinite state space. However, when  $c_r > 0$ , it is without loss of optimality to impose an upper bound  $M$  on the queue length and reject all incoming riders once the queue reaches this limit. Otherwise, allowing the queue to grow indefinitely would result in unbounded penalties in the objective. To find an optimal policy in a CTMDP, as outlined in Puterman (2014), a common approach is to transform it into a discrete-time MDP by using the *uniformization* method. However, to apply this method, the maximum transition rate among all states has to be bounded. Unfortunately, under the action space defined in Section 3, the transition rate can become *infinite* as multiple state transitions can occur instantaneously—e.g., if more than one dispatch action is triggered in succession. To bound the transition rates at each state, we must expand the action space. Upon each event, either a new rider request arrival or a trip completion, the platform makes a dispatch decision. Specifically, at each state, it must now determine *how many* drivers to dispatch in response to a rider arrival, and separately, *how many* to dispatch upon a trip completion. The formal definition of this new action space and the corresponding Bellman optimality equation are detailed in Appendix A.1.<sup>4</sup> Although this alternative action space guarantees bounded transition rates, it introduces significant redundancy: instead of a binary dispatch decision for each state, the action can now take any integer value up to the minimum of available riders and drivers, depending on future events. This added complexity makes it intractable. While one could restrict the action space to dispatching at most one driver at a time, we will show numerically in Section 5.1 that the problem remains computationally intensive for real-world instances. This motivates the need for alternative, efficient solution approaches, which we develop by leveraging the structural properties of our problem.

<sup>4</sup> Note that this new action space contains the action space defined in Section 3.1, nevertheless it can be shown that there always exists an optimal policy that is contained in both spaces. Consequently, they are equivalent from an optimization standpoint.

#### 4.1. Properties of the Optimal Dispatching Policies

We begin by analyzing the properties of optimal dispatching policies. Notably, given a dispatching policy, the pricing optimization problem can become simpler: it suffices to consider only the class of recurrent states under the specified dispatching policy  $\phi$ , which can be significantly smaller than the full state space (in fact, by an order of magnitude smaller under our later proposed dispatching policy). We first introduce a mild assumption on  $\mu$ .

ASSUMPTION 1. *We assume that  $\mu$  satisfies the following two conditions.*

- (1)  $l\mu_{l,m+1} - l\mu_{l,m}$  is non-increasing in  $m$  and non-decreasing in  $l$ ;
- (2)  $(l+1)\mu_{l+1,m} - l\mu_{l,m}$  is non-increasing in  $l$  and non-decreasing in  $m$ .<sup>5</sup>

Roughly speaking, Assumption 1 captures the idea of diminishing returns: adding an additional idle driver or waiting rider yields progressively smaller increments in service rate. In fact, Assumption 1 can be more easily understood by considering analogous monotonicity conditions on the differences of  $\mu_{l,m}$ , rather than  $l\mu_{l,m}$ , which is a *stronger* requirement that implies Assumption 1. For condition (1) on  $m$ , as rider queue length increases, the marginal impact of an additional waiting rider on pickup distance and service rate decreases. This is equivalent to the discrete concavity of  $l\mu_{l,m}$  in  $m$  for fixed  $l$ . For condition (1) on  $l$ , as the number of drivers in service  $l$  increases (and idle drivers  $L-l$  decrease), the marginal impact of an additional rider on service rate,  $\mu_{l,m+1} - \mu_{l,m}$ , increases, so as  $l\mu_{l,m+1} - l\mu_{l,m}$ . For condition (2), we focus on  $l$  since monotonicity in  $m$  mirrors that in  $l$  under condition (1). As  $l$  increases, the marginal impact of an additional idle driver,  $\mu_{l,m} - \mu_{l+1,m}$ , increases, implying that  $(l+1)\mu_{l+1,m} - l\mu_{l,m}$  decreases in  $l$ . This corresponds to the discrete concavity of  $l\mu_{l,m}$  in  $l$  for fixed  $m$ .<sup>6</sup>

We now proceed to discuss how we can derive an optimal dispatching policy under Assumption 1. We first classify a state into either type 1 or type 2, defined as follows.

DEFINITION 1 (STATE CLASSIFICATION). We classify a state  $(l, m) \in \mathcal{S}$  as *type 1* if its total service rate,  $l\mu_{l,m}$ , exceeds that at  $(l+1, m-1)$ , i.e.,  $l\mu_{l,m} > (l+1)\mu_{l+1,m-1}$ . If  $l = L$  or  $m = 0$ ,  $(l, m)$  is classified as a type 1 state as well. Otherwise, if  $l\mu_{l,m} \leq (l+1)\mu_{l+1,m-1}$ , we classify  $(l, m)$  as *type 2*.

<sup>5</sup> In fact,  $l\mu_{l,m+1} - l\mu_{l,m}$  being non-decreasing in  $l$  in condition (1) is equivalent to  $(l+1)\mu_{l+1,m} - l\mu_{l,m}$  being non-decreasing in  $m$  in condition (2). We keep both in the assumption for clarity.

<sup>6</sup> Assumption 1 may be compared to the joint discrete concavity of  $l\mu_{l,m}$  in both  $l$  and  $m$ . However, neither condition implies the other: joint concavity requires the Hessian matrix (formed by second forward differences) of  $l\mu_{l,m}$  to be negative semi-definite, whereas Assumption 1 is equivalent to requiring non-positive diagonal entries and non-negative off-diagonal entries in this Hessian.

In short, a type 1 state has a higher total service rate than its lower-left neighbor, the state reached by dispatching exactly one driver. Conversely, a type 2 state has a lower total service rate than its lower-left neighbor. The following lemma provides an important observation about the distribution of these two types of states.

LEMMA 2. *Suppose that  $\mu$  satisfies Assumption 1. Then the following statements hold.*

- (1) *If  $(l', m')$  is a type 1 state, then for any  $l \geq l'$  and  $m \leq m'$ ,  $(l, m)$  is also a type 1 state.*
- (2) *If  $(l', m')$  is a type 2 state, then for any  $l \leq l'$  and  $m \geq m'$ ,  $(l, m)$  is also a type 2 state.*

$l \backslash m$	$m' - 1$	$m'$	$l \backslash m$	$m' - 1$	$m'$
$l'$	$\dots$	$l' \mu_{l', m' - 1}$	$l'$	$\vdots$	$\vdots$
$l' + 1$	$\dots$	$(l' + 1) \mu_{l' + 1, m' - 1}$	$l' + 1$	$l' \mu_{l', m' - 1}$	$l' \mu_{l', m'}$
	$\angle$	$\angle$		$\not\approx$	$\not\approx$
	$\angle$	$\angle$		$(l' + 1) \mu_{l' + 1, m' - 1}$	$(l' + 1) \mu_{l' + 1, m'}$
	$\vdots$	$\vdots$		$\not\approx$	$\not\approx$
	$\vdots$	$\vdots$		$\dots$	$\dots$

- (a) States left or below a type 1 are type 1.      (b) States right or above a type 2 are type 2.

**Table 1** Illustration of Lemma 2. If the inequality shown in red is satisfied, then the inequalities shown in black are satisfied as well.

Lemma 2 implies that under Assumption 1, each anti-diagonal of the state map contains a state whose total service rate is greater than or equal to that of all other states along the same anti-diagonal. Intuitively, staying at states with high total service rates can improve system performance. Our main result below formalizes this.

THEOREM 1 (**Optimal Dispatching Policy**). *Suppose that  $\mu$  satisfies Assumption 1. Then, the following statements hold.*

- (1) *If  $c_d = c_r$ , there exists an optimal policy  $(\lambda^*, \phi^*)$  such that  $\phi^*(l, m) = 0$  for all type 1 states and  $\phi^*(l, m) = 1$  for all type 2 states.*
- (2) *If  $c_d > c_r$ , there exists an optimal policy  $(\lambda^*, \phi^*)$  such that  $\phi^*(l, m) = 0$  for all type 1 states.*
- (3) *If  $c_d < c_r$ , there exists an optimal policy  $(\lambda^*, \phi^*)$  such that  $\phi^*(l, m) = 1$  for all type 2 states.*

Theorem 1 characterizes the structure of the optimal dispatching policy  $(\lambda^*, \phi^*)$  based on the relationship between the driver and rider penalty coefficients  $c_d$  and  $c_r$ . Notably, when  $c_d = c_r$ —that is, when the difference between the driver’s in-service and idle costs equals the difference between the rider’s queueing and pickup waiting penalties ( $w_s^d - w_o^d = w_q^r - w_p^r$ )—the optimal dispatching policy admits a closed-form solution: after each dispatch, the system should be positioned along

the boundary between type 1 and type 2 states, at the state with the highest total service rate on the corresponding anti-diagonal. When  $c_d \neq c_r$ , the optimization simplifies to determining the dispatching policy for only one state type. Specifically, when  $c_d < c_r$ , the rider queueing penalty has a greater impact, so the platform should adopt an aggressive stance by dispatching drivers more readily to reduce rider wait times. Conversely, when  $c_d > c_r$ , driver penalty dominates, and the platform should take a more conservative approach by delaying dispatches and letting more riders to queue in order to reduce pick-up distances and associated driving costs. The proof relies on a series of coupling arguments, where we couple the system under an arbitrary policy with one governed by a deliberately constructed policy that satisfies the properties in Theorem 1. We then show that the constructed policy leads to a weakly better objective.

We conclude this subsection by noting that Theorem 1 also holds under any static pricing policy, where the effective arrival rate remains constant across all states.

REMARK 1. If the effective arrival rate is held constant across all states (i.e.,  $\lambda(l, m) = \bar{\lambda}$  for all  $l \in \mathcal{L}$  and  $m \in \mathbb{Z}_{\geq 0}$ ), an optimal dispatching policy still satisfies Theorem 1.

#### 4.2. Zigzag Dispatching Policy

When  $c_d = c_r$ , the optimal dispatching policy  $\phi^*$  described in Theorem 1 is characterized by a zigzag boundary that separates the regions where  $\phi^*(l, m) = 0$  and  $\phi^*(l, m) = 1$  (see Table 2a for an example). This observation motivates us to define a specific subclass of dispatching policies, which we refer to as *zigzag* policies. As we will show in subsequent sections, even without the condition  $c_d = c_r$  or Assumption 1, focusing on this subclass can substantially simplify computation while still yielding near-optimal solutions. We begin by formally defining a zigzag policy.

DEFINITION 2 (ZIGZAG POLICY). We say a dispatching policy is zigzag if:

- (1) For all  $l \in \mathcal{L}$ ,  $(\phi(l, m))_{m \in \mathbb{Z}_{\geq 0}}$  is a sequence of consecutive 0(s) followed by consecutive 1(s);
- (2) For all  $m \in \mathbb{Z}_{\geq 0}$ ,  $(\phi(l, m))_{l \in \mathcal{L}}$  is a sequence of consecutive 1(s) followed by consecutive 0(s).

If we interpret the policy as a matrix with rows indexed by  $l$  and columns by  $m$ , the definition of a zigzag policy closely resembles that of a matrix in row echelon form: all elements to the left of the leading entry in each row are zero, and each leading entry appears to the right of the leading entry in the row above. The key difference is that, in a zigzag policy, all nonzero entries are set to 1. Below, we provide examples of both zigzag and non-zigzag policies for illustration.

EXAMPLE 1 (ZIGZAG AND NON-ZIGZAG POLICIES). In Table 2, we consider a platform with a total of  $L = 4$  drivers. For  $m > 4$ , we keep the dispatching policy the same as the column with  $m = 4$ . Each element represents whether to make a dispatch under the corresponding state. Table 2a gives an example of a zigzag policy that meets both conditions outlined in Definition 2. In

$l \backslash m$	0	1	2	3	4	...
0	0	<b>0</b>	1	1	1	...
1	0	<b>0</b>	1	1	1	...
2	0	<b>0</b>	<b>0</b>	<b>0</b>	1	...
3	0	0	0	<b>0</b>	<b>0</b>	...
4	0	0	0	0	0	...

(a) Zigzag policy

$l \backslash m$	0	1	2	3	4	...
0	0	1	1	1	1	...
1	0	0	1	0	1	...
2	0	0	0	0	1	...
3	0	0	0	0	0	...
4	0	0	0	0	0	...

(b) Non-zigzag policy

$l \backslash m$	0	1	2	3	4	...
0	0	0	1	1	1	...
1	0	1	1	1	1	...
2	0	0	0	0	1	...
3	0	0	0	0	0	...
4	0	0	0	0	0	...

(c) Non-zigzag policy

**Table 2** Examples of zigzag and non-zigzag policies.

contrast, the policies depicted in Tables 2b and 2c are not zigzag policies. The policy depicted in Table 2b violates condition (1), while the policy depicted in Table 2c violates condition (2) in the definition.

Note that in the absence of Assumption 1 and  $c_r = c_d$ , there might not exist a zigzag policy within the set of optimal dispatching policies. In Appendix A.2, we provide a counterexample (Example 2). Nevertheless, focusing on zigzag policies offers both practical and analytical advantages. First, zigzag policies are easily interpretable as threshold policies: for a given number of drivers in service  $l$ , the policy specifies a dispatching threshold on the rider queue length  $m$ , so the platform dispatches whenever  $m$  exceeds this threshold. Conversely, for a given  $m$ , the policy sets a threshold on  $l$ , dispatching whenever  $l$  falls below this value. Second, zigzag policies are highly tractable, as the resulting Markov chain has a simple product-form stationary distribution, similar to that of a birth-death process, that enables closed-form evaluation of the objective. In our model, a birth refers to a rider joining the queue, and a death refers to a trip completion. Moreover, under a zigzag policy, the set of recurrent states traces out a *zigzag path* starting at a state with  $l = 0$ . This path serves as a boundary between regions of zeros and ones, for example,  $((0, 1), (1, 1), (2, 1), (2, 2), (2, 3), (3, 3), (3, 4), \dots)$  as highlighted in Table 2a. Since only recurrent states affect the system’s long-run behavior, we can focus our analysis only on states along a zigzag path. We now formally introduce the definition of a zigzag path, which will play a key role in the algorithm design.

**DEFINITION 3 (ZIGZAG PATH).** A zigzag path  $P = ((l_1, m_1), (l_2, m_2), \dots, (l_I, m_I))$  under a zigzag dispatching policy  $\phi$  is a sequence of states that satisfies:

- (1) (Origin)  $l_1 = 0$ ,  $\phi(0, m_1) = 0$  and  $\phi(0, m_1 + 1) = 1$ ;
- (2) (Monotonicity)  $l_{i+1} \geq l_i, m_{i+1} \geq m_i, \forall i \in \{1, \dots, I - 1\}$ ;
- (3) (Single movement)  $l_{i+1} + m_{i+1} - l_i - m_i = 1, \forall i \in \{1, \dots, I - 1\}$ .

In other words, a path is defined as a sequence of states, where each successive state is either one step to the right (i.e.,  $l_{i+1} = l_i$  and  $m_{i+1} = m_i + 1$ ), or one step down (i.e.,  $l_{i+1} = l_i + 1$  and  $m_{i+1} = m_i$ ) from the previous state. Given index  $i$ , the rightward step indicates  $\phi(l_i, m_i + 1) = 0$ , which means that the platform will not make a dispatch for a new rider arrival. However, it will dispatch a driver for a trip completion. Conversely, the downward step indicates  $\phi(l_i, m_i + 1) = 1$  and  $\phi(l_i + 1, m_i) = 0$ , which means that the platform will not make a dispatch upon a trip completion but will dispatch a driver upon a new rider arrival.

Each zigzag path  $P = ((l_1, m_1), (l_2, m_2), \dots, (l_I, m_I))$  defines a zigzag policy that terminates at state  $(l_I, m_I)$  by rejecting any new riders. The resulting stationary distribution can be computed in closed form using standard results for birth-death processes.

$$\pi(l_i, m_i) = \frac{\prod_{j=1}^i \frac{\lambda(l_j, m_j)}{l_j \mu_{l_j, m_j}}}{1 + \sum_{k=1}^I \prod_{j=1}^k \frac{\lambda(l_j, m_j)}{l_j \mu_{l_j, m_j}}}, \quad \forall i \in \{1, \dots, I\}. \quad (4)$$

**A Dynamic Programming (DP) Heuristic for Optimal Zigzag Policy.** Leveraging the properties of zigzag paths, we now present an efficient dynamic-programming-based heuristic algorithm that produces high-quality zigzag dispatching policies for general settings with arbitrary  $c_d, c_r > 0$ , without requiring Assumption 1. The algorithm starts at  $(0, 0)$ , iterates top to bottom through the first column ( $m = 0$ ), and then proceeds column by column, iteratively extending the zigzag path. When reaching an unvisited state  $(l, m)$ , the algorithm evaluates all zigzag paths terminating at that state, considering transitions from two possible directions: (1) from the left, where the previous state is  $(l, m - 1)$  (if  $m \geq 1$ ), and (2) from above, where the previous state is  $(l - 1, m)$  (if  $l \geq 1$ ). Enumerating all possible paths results in an exponential number of candidates in  $l$  and  $m$ . To address this, we introduce a *dominance condition* to prune suboptimal paths at each state. Specifically, in our framework, a zigzag path is said to dominate another terminating at the same state if, under the corresponding optimal pricing policy, its objective value is always greater for any future extensions. Consequently, dominated paths can be safely discarded, as they cannot contribute to the optimal zigzag dispatching policy. However, it is challenging to establish an exact dominance condition that guarantees only a polynomial or constant number of paths are retained at each state.<sup>7</sup> This difficulty arises because our objective is inherently path-dependent: when a

<sup>7</sup> For example, a sufficient set of exact dominance conditions for two zigzag paths terminating at the same state, path 1 dominates path 2, can be:

- (1) *Service rate dominance.* For every state  $(l, m)$  in path 2, the total service rate  $l\mu_{l,m}$  must be no greater than that of the state on path 1 lying on the same anti-diagonal (i.e., the state with the same  $l + m$  value);
- (2) *Penalty rate dominance.* For every state  $(l, m)$  in path 2, the total penalty rate  $c_d l + c_r m$  must be greater than or equal to that of the state on path 1 lying on the same anti-diagonal (i.e., the state with the same  $l + m$  value).

Although these criteria guarantee dominance, they are too stringent to be satisfied in numerical experiments.

zigzag path is extended by additional states, the marginal change in its objective value (under the optimal pricing policy) depends on the induced stationary distributions, which in turn depend on the entire sequence of states traversed (see equation (4)), rather than just the newly added state. This is in sharp contrast to stage-additive shortest-path problems, where edge costs are simply summed and classical dominance rules readily apply (such as those in Dijkstra’s algorithm); such rules do not hold in our setting.

Instead, we adopt a *heuristic* dominance rule: if one zigzag path achieves a higher objective value than another terminating at the same state, it is likely, though not guaranteed, that this dominance will persist when both paths are extended with identical future states. Based on this heuristic, at each state, we retain only the path with the higher objective value among those arriving from the left or from above, without considering the influence of future states. On the other hand, when we compute the objective of each zigzag path, its optimal pricing policy can be found by solving the corresponding Bellman equation using value iteration.<sup>8</sup> Although its stationary distribution admits a closed-form expression from equation (4), this approach can be computationally intensive, especially when used as a subroutine, since the prices for every state  $(l, m)$  along the zigzag path  $P$  must be optimized. To maintain efficiency, *static pricing* is often employed as an effective approximation (see, e.g., Besbes et al. 2022b and Bergquist and Elmachtoub 2024). Let  $\tilde{R}_s(\bar{\lambda}, P) := \sum_{(l,m) \in P} \pi(l, m) (\bar{\lambda} (p_0 + w_p^r t_0 + p_1(\bar{\lambda}) \cdot t_0) - c_{dl} - c_r m)$  be the objective value under zigzag path  $P$  and static arrival rate  $\bar{\lambda}$ . This quantity can be computed and optimized (using line search over  $\bar{\lambda}$ ) efficiently using the product-form distribution  $\pi(l, m)$  from equation (4).

The entire procedure is summarized in Algorithm 1. We construct a table  $P$ , where  $P_{l,m}$  records the best zigzag path terminating at state  $(l, m)$ . Notably, the update steps in Algorithm 1 naturally incorporate the option to terminate a zigzag path early by blocking all future arrivals beyond a certain queue length—implemented by setting the maximum price  $p_{\max}$ .<sup>9</sup> Accordingly, we maintain a matrix  $R$ , where  $R_{l,m}$  stores the best objective value under static pricing for zigzag paths that either terminate at  $(l, m)$  or are cut off prior to reaching  $(l, m)$ . At each state  $(l, m)$ , let  $P_{\text{above}}$  and  $P_{\text{left}}$  denote the zigzag paths that reach the current state by extending the best paths from the state above and the state to the left, respectively. Specifically, consider extending the path  $P_{l,m-1}$

<sup>8</sup> One could also directly optimize it using the closed-form expressions from equation (4) through a nonlinear optimization solver.

<sup>9</sup> Extending a path may decrease the objective value under static pricing, as the constraint of uniform pricing across all states can lead to large penalty terms. In such cases, the optimal static pricing may be a poor approximation of the optimal dynamic policy. Following the approach of Bergquist and Elmachtoub (2024), we consider applying the static price  $\bar{\lambda}$  only up to a designated cutoff state along the zigzag path. Beyond this cutoff, all subsequent arrivals are blocked by setting the maximum price  $p_{\max}$ .

vertically downward by one state  $(l, m)$ , denoted as  $P_{\text{above}}$ . Let  $\mathcal{R}_{\text{above}}$  be the maximum of the optimal objective value achieved by  $P_{\text{above}}$  under static pricing and  $R_{l, m-1}$ . If  $R_{l, m-1}$  is larger, this indicates that introducing a cutoff yields a higher objective, so extending  $P_{l, m-1}$  to  $P_{\text{above}}$  does not improve the objective value, and thus  $\mathcal{R}_{\text{above}} = R_{l, m-1}$ . Conversely, if  $R_{l, m-1}$  is smaller, no cutoff is imposed, and optimizing the static price along  $P_{\text{above}}$  increases the objective value; in this case,  $\mathcal{R}_{\text{above}} = \sup_{\bar{\lambda}} \tilde{\mathcal{R}}_s(\bar{\lambda}, P_{\text{above}})$ . The same reasoning applies for  $P_{\text{left}}$ . After that, we retain the path between  $P_{\text{above}}$  and  $P_{\text{left}}$  that has a higher objective value for  $P_{l, m}$ . If two paths have the same objective value, we break ties by selecting the one with the higher service rate—that is, we choose  $P_{\text{above}}$  if the service rate at  $(l-1, m)$  exceeds that at  $(l, m-1)$  (i.e., if  $(l-1, m)$  is a type 1 state); otherwise, we retain  $P_{\text{left}}$ .

As we briefly mentioned in Section 3, although the number of riders waiting in the queue can grow without limit, there naturally exists an upper bound  $M$  without loss of optimality due to the increasing rider waiting penalty. Proposition 1 below gives such a bound in the context of Algorithm 1 to facilitate an implementation with a finite number of iterations  $\mathcal{O}(ML)$ .

**PROPOSITION 1.** *If  $M \geq L\bar{\mu}p_{\max}/c_r$ , then Algorithm 1 will always yield the same objective value.*

After the algorithm terminates, we compute the optimal dynamic pricing policy  $\lambda^*$  using value iteration based on the dispatching policy generated by the zigzag path  $P_{L, M}$ . Theorem 2 demonstrates that, although Algorithm 1 is heuristic in nature, it recovers the optimal dispatching and pricing policies under Assumption 1 and  $c_d = c_r$ .

**THEOREM 2.** *Suppose  $\mu$  satisfies Assumption 1, and  $c_d = c_r$ . Algorithm 1 yields optimal dispatching and pricing policies  $(\phi^*, \lambda^*)$  such that  $\phi^*(l, m) = 0$  for all type 1 states and  $\phi^*(l, m) = 1$  for all type 2 states.*

## 5. Numerical Experiments

In this section, we demonstrate the effectiveness and efficiency of our proposed Algorithm 1 through extensive numerical experiments. In Section 5.1, we conduct synthetic experiments within our continuous-time Markovian model. In Section 5.2, we evaluate a range of dispatching and pricing policies in a simulated environment that incorporates real-world spatial features, relinquishing various modeling assumptions.

### 5.1. Synthetic Experiments

We conduct experiments based on our Markovian model, considering two scenarios with parameters  $(L, \Lambda, M) \in \{(20, 8, 10), (100, 40, 50)\}$ . Rider arrival locations and destinations are independently and uniformly sampled from a  $10 \times 10$  square service region, with distances calculated using the

---

**Algorithm 1** A DP Heuristic for Optimal Zigzag Policy

---

- 1: Create an  $(L + 1) \times (M + 1)$  table  $P$ , where  $P_{l,m}$  stores the best zigzag path terminated at  $(l, m)$ .
  - 2: Create an  $(L + 1) \times (M + 1)$  matrix  $R$ , where  $R_{l,m}$  stores the best objective value at  $(l, m)$ .
  - 3: Initialize  $P_{l,0} \leftarrow ((0,0), (1,0), \dots, (l,0))$  for all  $l \in \{0, 1, \dots, L\}$ ;  $P_{0,m} \leftarrow ((0,m))$  for all  $m \in \{1, 2, \dots, M\}$ .
  - 4: Initialize  $R_{0,m} \leftarrow 0$  for all  $m \in \{0, 1, \dots, M\}$ .
  - 5: **for**  $l = 1$  to  $L$  **do**
  - 6:      $R_{l,0} \leftarrow \max\{R_{l-1,0}, \sup_{\bar{\lambda}} \tilde{\mathcal{R}}_s(\bar{\lambda}, P_{l,0})\}$ .
  - 7: **end for**
  - 8: **for**  $m = 1$  to  $M$  **do**
  - 9:     **for**  $l = 1$  to  $L$  **do**
  - 10:         Construct two paths  $P_{\text{above}}$  and  $P_{\text{left}}$  by appending  $(l, m)$  to  $P_{l-1,m}$  and  $P_{l,m-1}$ , respectively.
  - 11:         Compute  $\mathcal{R}_{\text{above}} \leftarrow \max\{R_{l-1,m}, \sup_{\bar{\lambda}} \tilde{\mathcal{R}}_s(\bar{\lambda}, P_{\text{above}})\}$ .
  - 12:         Compute  $\mathcal{R}_{\text{left}} \leftarrow \max\{R_{l,m-1}, \sup_{\bar{\lambda}} \tilde{\mathcal{R}}_s(\bar{\lambda}, P_{\text{left}})\}$ .
  - 13:         **if**  $\mathcal{R}_{\text{left}} > \mathcal{R}_{\text{above}}$  **then**
  - 14:              $R_{l,m} \leftarrow \mathcal{R}_{\text{left}}, P_{l,m} \leftarrow P_{\text{left}}$ .
  - 15:         **else if**  $\mathcal{R}_{\text{left}} < \mathcal{R}_{\text{above}}$  **then**
  - 16:              $R_{l,m} \leftarrow \mathcal{R}_{\text{above}}, P_{l,m} \leftarrow P_{\text{above}}$ .
  - 17:         **else if**  $\mathcal{R}_{\text{left}} = \mathcal{R}_{\text{above}}$  **then**
  - 18:              $R_{l,m} \leftarrow \mathcal{R}_{\text{left}}, P_{l,m} \leftarrow \begin{cases} P_{\text{above}}, & \text{if } (l-1, m) \text{ is a type 1 state.} \\ P_{\text{left}}, & \text{if } (l-1, m) \text{ is a type 2 state.} \end{cases}$
  - 19:         **end if**
  - 20:     **end for**
  - 21: **end for**
  - 22: Compute the optimal dynamic pricing policy  $\lambda^*$  under zigzag path  $P_{L,M}$ .
  - 23: **Output:** The dispatching policy yielded by zigzag path  $P_{L,M}$  and the corresponding pricing policy  $\lambda^*$ .
- 

Euclidean norm. All distances and times are measured in kilometers and minutes, respectively. We assume drivers travel in unit speed. The service rate  $\mu_{l,m}$  is estimated via Monte Carlo sampling: specifically, we uniformly sample the locations of  $L - l$  idle drivers and  $m$  riders within the service region, and, at each dispatch event, employ a nearest-neighbor strategy that matches the closest rider-driver pair. This sampling procedure is repeated 100,000 times for each  $(l, m)$ , and the average pickup time is computed. Finally, we estimate  $\mu_{l,m}$  as the reciprocal of the sum of the average trip time and the average pickup time.<sup>10</sup> The average trip time  $t_0$  is taken as the expected distance between two uniformly sampled points in the  $10 \times 10$  square, which can be computed as  $t_0 = \frac{2}{3} (2 + \sqrt{2} + 5 \ln(1 + \sqrt{2})) \approx 5.2$ . We specify the inverse demand function using a linear model,

<sup>10</sup> Our estimated service rates satisfy Assumption 1 for all states  $(l, m)$  except  $(1, 1)$  and  $(0, 2)$ . Since these states have negligible stationary probabilities, their exceptions have little impact on optimization.

$p_1(\lambda) = 2(1 - \lambda/\Lambda)$ , and set  $p_0 + w_p^r t_0 = 5$ . In this setting, the base fare per trip  $p_0$  is approximately \$4, the per-minute penalty for rider pickup waiting is  $w_p^r = 0.2$ , and the maximum per-kilometer price  $p_{\max}$  is \$2—consistent with those commonly observed on ride-hailing platforms.

We test  $3 \times 3 = 9$  combinations of  $c_d$  and  $c_r$  by taking  $c_d \in \{0.5, 0.75, 1.0\}$  and  $c_r \in \{0.5, 0.75, 1.0\}$ . In each scenario, we evaluate the performance of our zigzag policy, optimized using Algorithm 1, by comparing it against two benchmark policies.

1. **Value Iteration:** We apply value iteration to solve objective (3) using the alternative action space introduced at the beginning of Section 4. As previously discussed, the full action space, which permits dispatching multiple drivers simultaneously, is computationally intractable. Therefore, we restrict the action space to allow dispatching at most one driver at a time. More details can be found in Appendix A.1.
2. **Greedy Dispatching Policy:** A baseline policy that always dispatches a driver whenever one is available, with the dynamic pricing policy subsequently optimized via value iteration.

$c_d, c_r$	Value Iteration		Greedy, Dyn.		Zigzag, Dyn.		Zigzag, Sta.	
	$\tilde{\mathcal{R}}(\lambda, \phi)$	Runtime (s)	$\tilde{\mathcal{R}}(\lambda, \phi)$	Runtime (s)	$\tilde{\mathcal{R}}(\lambda, \phi)$	Runtime (s)	$\tilde{\mathcal{R}}_s(\lambda, \phi)$	Runtime (s)
0.5, 0.5	20.54	544.79	18.32	20.39	20.54	16.56	20.11	1.69
0.5, 0.75	19.67	514.68	17.53	26.11	19.67	15.90	19.21	1.67
0.5, 1.0	19.05	469.02	17.25	19.03	19.05	14.73	18.53	1.52
0.75, 0.5	16.36	572.13	13.61	37.42	16.36	17.51	16.04	1.65
0.75, 0.75	15.57	525.36	13.46	23.30	15.57	16.43	15.24	1.60
0.75, 1.0	15.02	466.05	13.45	15.77	15.02	15.08	14.65	1.46
1.0, 0.5	12.44	591.52	10.06	21.21	12.43	18.21	12.23	1.45
1.0, 0.75	11.74	511.15	10.06	14.09	11.74	16.47	11.53	1.42
1.0, 1.0	11.26	451.86	10.06	12.32	11.26	14.79	11.03	1.27

**Table 3** Comparison of different algorithms under parameters  $(L, \Lambda, M) = (20, 8, 10)$ .

Tables 3 and 4 present results for two scenarios,  $(L, \Lambda, M) \in \{(20, 8, 10), (100, 40, 50)\}$ , respectively. We evaluate two pricing strategies derived from the zigzag policy produced by Algorithm 1: a static pricing policy (“Zigzag, Sta.”) and a dynamic pricing policy (“Zigzag, Dyn.”). Both zigzag policies consistently outperform the greedy benchmark. In Table 3, where value iteration can reach optimality within the time limit, “Zigzag, Dyn.” attains nearly identical objective values but with substantially lower computation time. Notably, when  $c_d = c_r$ , “Zigzag, Dyn.” matches the objective value of value iteration exactly, confirming its optimality as established in Theorem 2. For the larger scenario in Table 4, value iteration fails to converge within the time limit and yields

$c_d, c_r$	Value Iteration		Greedy, Dyn.		Zigzag, Dyn.		Zigzag, Sta.	
	$\tilde{\mathcal{R}}(\lambda, \phi)$	Runtime (s)	$\tilde{\mathcal{R}}(\lambda, \phi)$	Runtime (s)	$\tilde{\mathcal{R}}(\lambda, \phi)$	Runtime (s)	$\tilde{\mathcal{R}}_s(\lambda, \phi)$	Runtime (s)
0.5, 0.5	112.13	1,200.00	116.10	411.35	128.17	488.77	126.96	167.91
0.5, 0.75	101.42	1,200.00	111.20	1,200.00	125.78	658.32	124.36	168.83
0.5, 1.0	91.05	1,200.00	111.18	485.99	124.00	445.39	122.42	151.18
0.75, 0.5	88.05	1,200.00	91.11	1,200.00	105.41	573.68	104.67	169.17
0.75, 0.75	77.16	1,200.00	90.80	412.81	103.33	525.72	102.46	168.77
0.75, 1.0	66.64	1,200.00	90.80	266.46	101.76	460.57	100.80	152.40
1.0, 0.5	64.02	1,200.00	71.37	461.67	83.52	554.08	83.18	150.50
1.0, 0.75	52.93	1,200.00	71.37	273.75	81.76	527.70	81.35	150.32
1.0, 1.0	42.32	1,200.00	71.37	283.30	80.43	475.77	79.97	130.77

**Table 4** Comparison of different algorithms under parameters  $(L, \Lambda, M) = (100, 40, 50)$ . A 20-minute cap is imposed on every run; any runtime that exceeds this limit is reported as 1200.00 seconds.

solutions inferior to even the greedy policy. In Appendix A.3, we present and discuss additional performance metrics, including the average price per rider, revenue rate, average pickup time, and average queueing time, under the same experimental setup.

## 5.2. Simulation Experiments

We further validate our findings by implementing the algorithm in a simulated environment that reflects real-world ride-hailing spatial dispatching. In this simulation, we set  $(L, \Lambda, M) = (100, 40, 50)$  and again consider a  $10 \times 10$  square region where rider pick-up and drop-off locations are uniformly distributed. Idle drivers remain at their drop-off locations and do not reposition. Departing from the previous synthetic experiments, which assumed independently and state-dependent exponentially distributed service times, this simulation introduces service times that are correlated across dispatches due to driver and waiting rider locations and are endogenously sampled by the actual matching distance, which itself depends on the dispatching and pricing policies.

**5.2.1. Estimation of Service Rate.** Instead of estimating the service rate  $\mu$  based on randomly generated rider and driver locations, as in Section 5.1, we now estimate  $\mu$  directly from dispatching outcomes observed in simulation. We begin by simulating the system under a *constant-radius* dispatching policy: only the closest rider-driver pair within a radius  $r$  is dispatched, generating samples for analysis. A static pricing policy with a fixed effective arrival rate  $\lambda(l, m) = 12$  is applied uniformly across all states. We conduct 24 simulation runs with dispatching radii  $r \in \{0.5, 1, 1.5, \dots, 12\}$ , each over a time period of  $T = 20,000$ . During each run, we record the

pick-up times for every dispatch. Specifically, whenever the system enters state  $(l, m)$  and the next event is either an arrival or a trip completion immediately followed by a dispatch, we attribute the corresponding pickup time to state  $(l, m)$ . The average pickup time for each state is then computed across all simulation runs, with each average used as a data point for regression analysis. To mitigate sampling noise, states with fewer than 10 recorded samples are excluded from the dataset.

Following Wang et al. (2024), we model the average pickup time as a power-law function of the number of waiting riders in the queue and the number of idle drivers. Specifically, the average pickup time  $\eta_{l,m}$  in state  $(l, m)$  is estimated as:<sup>11</sup>

$$\eta_{l,m} = C \cdot (m + 1)^{\alpha_1} \cdot (L - l + 1)^{\alpha_2} \tag{5}$$

where  $C > 0$  and  $\alpha_1, \alpha_2 < 0$  are some constants. The right-hand side of Equation (5) takes the form of a Cobb–Douglas production function (Cobb and Douglas 1928). We then perform a log-log regression. In specific, the regression is based on the mean function  $\log \eta_{l,m} = \log C + \alpha_1 \log(m + 1) + \alpha_2 \log(L - l + 1)$ .

	coef	std. error	P >  t	[0.025	0.975]
$\hat{C}$	3.839	0.017	0.000	3.743	3.939
$\hat{\alpha}_1$	-0.274	0.004	0.000	-0.267	-0.282
$\hat{\alpha}_2$	-0.192	0.003	0.000	-0.186	-0.199

**Table 5** Regression results for covariates  $\alpha_1$ ,  $\alpha_2$ , and  $C$ .

The regression results are summarized in Table 5. We observe that the estimated coefficients,  $\hat{\alpha}_1$  and  $\hat{\alpha}_2$ , are significantly larger than the values of approximately  $-0.5$  reported when riders and drivers are uniformly distributed in space (see values reported in Yan et al. 2020 and Wang et al. 2024). This discrepancy is likely attributable to the correlation introduced by driver and waiting rider locations across dispatches. The service rate  $\mu_{l,m}$  can then be approximated as the reciprocal of the sum of the estimated expected pickup time at state  $(l, m)$  and the expected trip time  $t_0$ , i.e.,  $\hat{\mu}_{l,m} = 1/(\hat{\eta}_{l,m} + t_0)$ .

**PROPOSITION 2.** *If the fitted coefficient  $\hat{C} \leq t_0$ , then  $\hat{\mu}$  satisfies Assumption 1, and is strictly increasing in  $m$  and strictly decreasing in  $l$ .*

<sup>11</sup> There exists an expected pickup time at states where  $l = L$  or  $m = 0$  and  $l > 0$ , as some riders are still being served in these states. We thus add 1 to both  $m$  and  $L - l$  in equation (5).

Proposition 2 establishes that  $\hat{\mu}$  satisfies our assumptions provided that the expected pickup time at  $(l, m) = (0, 0)$  does not exceed  $t_0$ ; that is, the expected pickup time for a single waiting rider and a single available driver must be no greater than the expected trip time  $t_0$ . Our regression yields  $\hat{C} = 3.839$ , which is well below  $t_0 \approx 5.2$ . Thus, the estimated  $\hat{\mu}$  satisfies Assumption 1 with a comfortable margin.

**5.2.2. Simulation Results.** We compare the following dispatching and pricing policies over a simulated time period of  $T = 20,000$ :

1. *Constant radius dispatching, static pricing:* The platform dispatches the nearest driver-rider pair whenever their distance is less than or equal to a specified threshold  $\bar{r}$ , and applies a static price (effective arrival rate)  $\bar{\lambda}$ . We employ simulation optimization with coordinate ascent to jointly determine the optimal values of  $\bar{r}$  and  $\bar{\lambda}$ .
  - (a) We first determine  $\bar{r}$  through a line search with a step size of 0.2 under  $\bar{\lambda} = 12$  by running the simulation.
  - (b) Fixing the  $\bar{r}$  from step (a), we update  $\bar{\lambda}$  using line search with a step size of 0.2 by running the simulation.
  - (c) We repeat the above steps until the absolute differences between consecutive values of  $\bar{r}$  and  $\bar{\lambda}$  are less than or equal to 0.2.
2. *Zigzag dispatching, static pricing:* We adopt the zigzag dispatching policy from Algorithm 1, computed using the estimated service rates  $\hat{\mu}$  from Section 5.2.1. We use the corresponding optimal static pricing policy based on this dispatching policy.
3. *Zigzag dispatching, dynamic pricing:* We adopt the same zigzag dispatching policy as in (2), but instead apply the corresponding optimal dynamic pricing policy.

It is important to note that, in contrast to the constant radius policy, computing both zigzag policies does *not* require access to the simulation environment other than the calibrated service rate  $\hat{\mu}$ . Table 6 shows the objective and average pricing per ride for various algorithms under different  $c_d$  and  $c_r$ , averaged over the simulation period. In specific, the average price is computed as  $\sum_{(l,m) \in \mathcal{S}} \pi_{\lambda, \phi}(l, m) (p_0 + p_1(\lambda(l, m)) \cdot t_0)$ . Several observations can be drawn from the table. First, the performance of the two zigzag policies is comparable to that of the constant radius policy, even though the latter directly optimizes its parameters using the same simulation as in the evaluation. Second, dynamic pricing slightly outperforms static pricing under the same zigzag dispatching policy, while also yielding lower average prices. Table 7 further reports the average revenue per unit time, average pickup time, and average queueing time under varying values of  $c_d$  and  $c_r$ .

It is worth noting that the two tested zigzag dispatching policies make decisions on dispatching or not based solely on the counts of riders and drivers, without utilizing any spatial information

		C.R.		Zigzag, Sta.		Zigzag, Dyn.	
$c_d$	$c_r$	Obj.	Price	Obj.	Price	Obj.	Price
0.50	0.50	114.04	10.68	113.01	10.82	113.49	10.74
0.50	0.75	111.25	10.84	110.55	10.90	111.18	10.81
0.50	1.00	109.45	10.94	108.89	10.97	109.68	10.86
0.75	0.50	90.91	10.84	90.67	10.90	90.96	10.82
0.75	0.75	89.12	10.94	88.70	10.99	89.01	10.90
0.75	1.00	87.85	11.05	87.38	11.05	87.78	10.95
1.00	0.50	69.68	11.05	69.43	11.04	69.55	10.98
1.00	0.75	68.24	11.15	67.92	11.13	68.12	11.06
1.00	1.00	67.47	11.25	67.03	11.19	67.20	11.11

**Table 6** Objective values and average prices under different policies in simulation across various  $(c_d, c_r)$  settings.

		C.R.			Zigzag, Sta.			Zigzag, Dyn.		
$c_d$	$c_r$	Revenue	Pickup	Queue	Revenue	Pickup	Queue	Revenue	Pickup	Queue
0.50	0.50	152.12	1.33	0.89	148.58	1.32	0.73	149.44	1.37	0.68
0.50	0.75	147.81	1.43	0.53	145.98	1.38	0.52	147.08	1.44	0.48
0.50	1.00	144.89	1.50	0.36	144.17	1.42	0.41	145.50	1.50	0.37
0.75	0.50	147.92	1.35	0.60	146.09	1.27	0.63	147.32	1.31	0.60
0.75	0.75	144.88	1.33	0.46	143.54	1.32	0.45	144.98	1.37	0.42
0.75	1.00	141.85	1.38	0.30	141.70	1.35	0.35	143.39	1.42	0.32
1.00	0.50	141.88	1.22	0.46	141.95	1.20	0.54	143.10	1.22	0.51
1.00	0.75	138.67	1.27	0.30	139.38	1.24	0.39	140.82	1.27	0.36
1.00	1.00	135.43	1.23	0.25	137.57	1.27	0.30	139.27	1.30	0.28

**Table 7** Comparison of different policies in terms of revenue rate, average pickup time, and average queueing time in simulation across various  $(c_d, c_r)$  settings.

about their locations. This raises a question of how these policies might be improved if additional information, such as pickup distance, were incorporated into the dispatching policy. In Online Appendix A.4, we introduce a hybrid approach, referred to as the “two-radius policy,” which combines the zigzag and radius-based dispatching strategies. The two-radius policy consistently achieves higher objective values than the constant radius policy.

**5.2.3. Robustness Evaluation.** To further assess the robustness of our algorithm under varying environmental conditions, we evaluate the policies across a range of values for  $\Lambda \in$

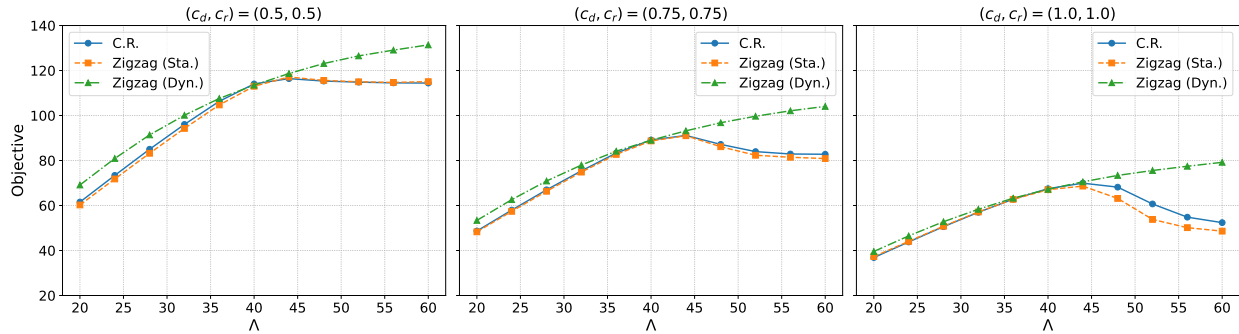


**Figure 1** Robustness of different policies when rider arrival rate  $\Lambda$  used in simulation deviates from the training value  $\Lambda = 40$ .

$\{20, 24, \dots, 60\}$  in the simulation and examine how deviations from the training scenario ( $\Lambda = 40$ ) impact policy performance.

Figure 1 presents the objective values of various algorithms across a range of rider arrival rates in simulation. While all three algorithms exhibit similar performance at the training arrival rate ( $\Lambda = 40$ ), their performance diverges as the actual  $\Lambda$  deviates from this value. The zigzag policy with dynamic pricing consistently improves its objective value as  $\Lambda$  increases and outperforms the other policies across all deviated  $\Lambda$  values. In contrast, the other two policies, both relying on static pricing, show greater variability and a decline in objective value when  $\Lambda > 40$ , despite rising demand. These results underscore the robustness of dynamic pricing, consistent with similar observations in Banerjee et al. (2015). It is also important to note that directly optimizing a dynamic pricing policy  $\lambda$  through simulation optimization is intractable due to its high dimension, which further highlights the value of our MDP framework.

## 6. Conclusion

In this paper, we analyze a Markov model that approximates the rider queuing and pickup processes in ride-hailing/robotaxi platforms with a fixed number of drivers. We incorporate state-dependent service times to capture key spatial matching characteristics. The platform optimizes net profit, penalized by rider waiting, through adaptive pricing and dispatching decisions that are state-dependent. We show that, under mild assumptions, the optimal dispatching policy admits a closed-form expression with a zigzag structure—interpretable as a monotone threshold-type policy—and is tractable for price optimization thanks to the resulting closed-form stationary distribution. Building on this insight, we propose an efficient and scalable dynamic programming heuristic to approximate the optimal zigzag policy in more general settings.

Synthetic experiments demonstrate that our algorithm achieves near-optimal performance and excellent scalability. We further validate our approach in a simulated ride-hailing dispatching and

pricing environment that captures features real-world spatial matching. The results show that the zigzag policy, computed without access to the simulation, performs comparably to a constant radius dispatching policy that is fine-tuned using the simulation environment. These findings highlight the promising applicability of the proposed zigzag policy in practice.

## References

- Balkanski E, Faenza Y, Périvier N (2023) The power of greedy for online minimum cost matching on the line. *Proceedings of the 24th ACM Conference on Economics and Computation*, 185–205, EC '23 (New York, NY, USA: Association for Computing Machinery).
- Banerjee S, Johari R, Riquelme C (2015) Pricing in ride-sharing platforms: A queueing-theoretic approach. *Proceedings of the Sixteenth ACM Conference on Economics and Computation*, 639, EC '15 (New York, NY, USA: Association for Computing Machinery).
- Benjaafar S, Wang Z, Yang X (2025) Human in the loop automation: Ride-hailing with remote (tele-)drivers. *Management Science* 71(3):2527–2543.
- Bergquist J, Elmachtoub AN (2024) Static pricing guarantees for queueing systems. URL <https://arxiv.org/abs/2305.09168>.
- Besbes O, Castro F, Lobel I (2022a) Spatial capacity planning. *Operations Research* 70(2):1271–1291.
- Besbes O, Elmachtoub AN, Sun Y (2022b) Technical note—static pricing: Universal guarantees for reusable resources. *Operations Research* 70(2):1143–1152.
- Castillo JC, Knoepfle D, Weyl EG (2025) Matching and pricing in ride hailing: Wild goose chases and how to solve them. *Management Science* 71(5):4377–4395.
- Chen M, Hu M (2025) (de)pooling eases spatial mismatch. Available at SSRN 5207578 .
- Cobb CW, Douglas PH (1928) A theory of production. *The American Economic Review* 18(1):139–165.
- Elmachtoub AN, Shi J (2025) *The Power of Static Pricing for Reusable Resources*, 357. EC '25 (New York, NY, USA: Association for Computing Machinery).
- Feng G, Kong G, Wang Z (2021) We are on the way: Analysis of on-demand ride-hailing systems. *Manufacturing & Service Operations Management* 23(5):1237–1256.
- Kanoria Y (2022) Dynamic spatial matching. *Proceedings of the 23rd ACM Conference on Economics and Computation*, 63–64, EC '22 (New York, NY, USA: Association for Computing Machinery).
- Puterman ML (2014) *Markov Decision Processes: Discrete Stochastic Dynamic Programming* (John Wiley & Sons).
- Wang G, Zhang H, Zhang J (2024) On-demand ride-matching in a spatial model with abandonment and cancellation. *Operations Research* 72(3):1278–1297.

Xu Z, Yin Y, Ye J (2020) On the supply curve of ride-hailing systems. *Transportation Research Part B: Methodological* 132:29–43.

Yan C, Zhu H, Korolko N, Woodard D (2020) Dynamic pricing and matching in ride-hailing platforms. *Naval Research Logistics (NRL)* 67(8):705–724.

## Appendix A: Additional Results

### A.1. An Alternative Definition of Action Space

In this section, we describe how the action space can be redefined to enable the use of uniformization in solving the objective in equation (3). To transform the continuous-time system into an equivalent discrete-time framework, it is necessary to bound the transition rate in each state. At state  $(l, m)$ , we redefine the dispatching action as  $(d_a(l, m), d_c(l, m))$ , where  $d_a(l, m)$  and  $d_c(l, m)$  denote respectively, the number of drivers to dispatch when the next event is a new rider joining the queue, or a trip completion, at state  $(l, m)$ . Since the number of dispatches cannot exceed the number of idle drivers and the number of riders in the queue at any state, the number of dispatches at state  $(l, m)$  follows  $d_a(l, m) \in \{0, 1, \dots, \min\{L - l, m + 1\}\}$  and  $d_c(l, m) \in \{0, 1, \dots, \min\{L - l + 1, m\}\}$ . If the next event is an effective rider arrival, the state transitions to  $(l + d_a(l, m), m + 1 - d_a(l, m))$ . Conversely, if the next event is a trip completion, the state transitions to  $(l - 1 + d_a(l, m), m - d_c(l, m))$ . Under this new action space, the transition rate at each state is bounded by  $M_0 := \max_{l, m} \{l\mu_{l, m}\} + \Lambda$ . Consequently, the Bellman optimality equation for the average reward MDP can be written as

$$\begin{aligned} \max_{\substack{\lambda(l, m) \in [0, \Lambda], \\ 0 \leq d_a(l, m) \leq \min\{L - l, m + 1\}, \\ 0 \leq d_c(l, m) \leq \min\{L - l + 1, m\}, \\ d_a(l, m), d_c(l, m) \in \mathbb{Z}_{\geq 0}}} & \left\{ \underbrace{\frac{\lambda(l, m)}{M_0} \left( p_0 + w_p^r t_0 + p_1(\lambda(l, m)) + h^*(l + d_a(l, m), m + 1 - d_a(l, m)) - h^*(l, m) \right)}_{\text{expected additional return under a new rider arrival}} \right. \\ & \left. + \underbrace{\frac{l\mu_{l, m}}{M_0} \left( h^*(l - 1 + d_c(l, m), m - d_c(l, m)) - h^*(l, m) \right)}_{\text{expected additional return under a trip completion}} - \underbrace{\frac{c_d l + c_r m}{M_0}}_{\text{penalty}} \right\} = g^*. \end{aligned} \quad (6)$$

In equation (6),  $g^*$  refers to the long-term average reward rate (revenue rate minus penalty rate) under the optimal policy. The bias term  $h^*(l, m)$  refers to the difference in the long-run expected total reward gained by starting the process at state  $(l, m)$  compared to starting the process with its steady-state distribution under an optimal policy. An optimal policy can be obtained by recovering the optimal solution of (6). One can solve (6) using relative value iteration (see Chapter 8 of Puterman 2014) under an average reward setting.

### A.2. Sub-optimality of the Zigzag Policy

EXAMPLE 2 (SUB-OPTIMALITY OF THE ZIGZAG POLICY CLASS). Table 8 gives an example where the optimal policy is non-zigzag. In this example,  $p_1(\cdot)$  is constant. We set  $c_d = c_r = 0.1$ . Table 8a gives the service rate  $\mu$  at each state, which does not satisfy Assumption 1. Table 8b shows the corresponding optimal dispatching policy, which does not follow a zigzag pattern. We compare this optimal dispatching policy with the optimal zigzag policy in Table 8c to show why it is strictly better. We consider a coupling between systems under the two policies (we use system (b) and system (c) to represent the systems under the optimal dispatching policy and the optimal zigzag policy, respectively). We couple all random events until both systems reach state  $(2, 2)$  and make different dispatching decisions. We keep both systems the same effective arrival rate during coupling. At that state, the optimal dispatching policy chooses not to dispatch while the optimal zigzag policy dispatches a driver. As a consequence, system (c) dispatches and moves to state  $(3, 1)$ ,

whereas system (b) stays in state (2, 2). One of the following three events can occur next: (1) a new rider arrival to both systems; (2) a trip completion in both systems; (3) a trip completion in system (b) only. Event (3) is possible to happen because the total service rate at state (2, 2) ( $2\mu_{2,2} = 4$ ) exceeds one at state (3, 1) ( $3\mu_{3,1} = 3$ ). If event (1) or (2) occurs, the two systems return to the same state, and the coupling is maintained. If event (3) occurs, system (b) completes an extra trip (relative to system (c)). At that point, system (b) is at (3, 0) and system (c) is at (3, 1). Then system (b) will keep having the same throughput rate but smaller penalty rate until there is an additional trip completion for system (c) compared to system (b). After that occurs, systems (b) and (c) lie on the same anti-diagonal (i.e., both systems have the same value of  $l + m$ ). Then either systems b and c are at the same state or system b is at (2, 2) and system c is at (3, 1). Both cases return to the situation we discussed before. Hence, during the coupling period, the throughput rate in both systems keeps the same, but system (b) has a lower average penalty rate, which shows the optimal zigzag policy is indeed sub-optimal.

<table border="1" style="border-collapse: collapse; text-align: center;"> <tr><td style="border: none;"><math>m \backslash l</math></td><td style="border: none;">0</td><td style="border: none;">1</td><td style="border: none;">2</td><td style="border: none;">3</td><td style="border: none;">...</td></tr> <tr><td style="border: none;">0</td><td>0</td><td>0</td><td>0</td><td>0</td><td>...</td></tr> <tr><td style="border: none;">1</td><td>1</td><td>1</td><td>2</td><td>2</td><td>...</td></tr> <tr><td style="border: none;">2</td><td>1</td><td>1</td><td>2</td><td>2</td><td>...</td></tr> <tr><td style="border: none;">3</td><td>1</td><td>1</td><td>2</td><td>2</td><td>...</td></tr> </table>	$m \backslash l$	0	1	2	3	...	0	0	0	0	0	...	1	1	1	2	2	...	2	1	1	2	2	...	3	1	1	2	2	...	<table border="1" style="border-collapse: collapse; text-align: center;"> <tr><td style="border: none;"><math>m \backslash l</math></td><td style="border: none;">0</td><td style="border: none;">1</td><td style="border: none;">2</td><td style="border: none;">3</td><td style="border: none;">...</td></tr> <tr><td style="border: none;">0</td><td>0</td><td>1</td><td>1</td><td>1</td><td>...</td></tr> <tr><td style="border: none;">1</td><td>0</td><td>1</td><td>1</td><td>1</td><td>...</td></tr> <tr><td style="border: none;">2</td><td>0</td><td>1</td><td>0</td><td>1</td><td>...</td></tr> <tr><td style="border: none;">3</td><td>0</td><td>0</td><td>0</td><td>0</td><td>...</td></tr> </table>	$m \backslash l$	0	1	2	3	...	0	0	1	1	1	...	1	0	1	1	1	...	2	0	1	0	1	...	3	0	0	0	0	...	<table border="1" style="border-collapse: collapse; text-align: center;"> <tr><td style="border: none;"><math>m \backslash l</math></td><td style="border: none;">0</td><td style="border: none;">1</td><td style="border: none;">2</td><td style="border: none;">3</td><td style="border: none;">...</td></tr> <tr><td style="border: none;">0</td><td>0</td><td>1</td><td>1</td><td>1</td><td>...</td></tr> <tr><td style="border: none;">1</td><td>0</td><td>1</td><td>1</td><td>1</td><td>...</td></tr> <tr><td style="border: none;">2</td><td>0</td><td>1</td><td>1</td><td>1</td><td>...</td></tr> <tr><td style="border: none;">3</td><td>0</td><td>0</td><td>0</td><td>0</td><td>...</td></tr> </table>	$m \backslash l$	0	1	2	3	...	0	0	1	1	1	...	1	0	1	1	1	...	2	0	1	1	1	...	3	0	0	0	0	...
$m \backslash l$	0	1	2	3	...																																																																																							
0	0	0	0	0	...																																																																																							
1	1	1	2	2	...																																																																																							
2	1	1	2	2	...																																																																																							
3	1	1	2	2	...																																																																																							
$m \backslash l$	0	1	2	3	...																																																																																							
0	0	1	1	1	...																																																																																							
1	0	1	1	1	...																																																																																							
2	0	1	0	1	...																																																																																							
3	0	0	0	0	...																																																																																							
$m \backslash l$	0	1	2	3	...																																																																																							
0	0	1	1	1	...																																																																																							
1	0	1	1	1	...																																																																																							
2	0	1	1	1	...																																																																																							
3	0	0	0	0	...																																																																																							
(a) Service rate $\mu$ at each state	(b) Optimal dispatching policy	(c) Optimal zigzag policy																																																																																										

**Table 8** Example of the sub-optimality for zigzag dispatching policies. For all  $m > 3$ , column  $m$  is identical to column 3.

### A.3. Additional Performance Metrics in Synthetic Experiments

We provide some additional performance metrics including average price for each rider, revenue rate, average pickup time, and average queueing time under the experiment setting in Section 5.1. Tables 9 and 10 show the relevant metrics under scenarios  $(L, \Lambda, M) = (20, 8, 10)$  and  $(L, \Lambda, M) = (100, 40, 50)$ , respectively. When  $(L, \Lambda, M) = (20, 8, 10)$ , all metrics in the zigzag policy under dynamic pricing is close to ones derived from the value iteration. By contrast, the greedy policy yields significantly larger pickup times and shorter queueing times compared to other policies. Under the zigzag policy, static pricing results in a higher average price and comparable pickup time but leads to longer queueing times compared to dynamic pricing. This is because static pricing lacks the ability to adaptively dampen demand as congestion builds, causing the system to rely more heavily on queueing.

### A.4. Two-radius Policy

We integrate our zigzag policy with constant-radius dispatching and refer to the resulting approach as the “two-radius policy”. This policy is implemented as follows.

1. *Two-radius dispatching, static pricing:* We adopt policy 2 (“Zigzag, Sta.”) described in Section 5.2.2 and introduce a modification to the dispatching rule. Specifically, we define two threshold radii,  $r_0$  and  $r_1$ . Under the zigzag policy  $\phi(l, m) = i \in \{0, 1\}$ , the platform dispatches a driver if the pickup distance is less than or equal to  $r_i$ . We set  $r_0 = r^* - \delta$  and  $r_1 = r^* + \delta$ , where  $r^*$  is the optimal constant radius identified in policy 1 (C.R.) in Section 5.2.2. The optimal value of  $\delta$  is determined by performing a line search with a step size of 0.2 using simulation.

		Value Iteration				Greedy, Dyn.			
$c_d$	$c_r$	Revenue	Price	Pickup	Queue	Revenue	Price	Pickup	Queue
0.50	0.50	28.30	10.86	1.36	1.53	27.41	10.93	2.55	1.65
0.50	0.75	27.59	11.00	1.47	1.18	25.70	11.36	2.79	0.89
0.50	1.00	26.86	11.12	1.67	0.86	23.73	11.60	2.77	0.26
0.75	0.50	27.74	11.01	1.23	1.50	24.84	11.43	2.55	0.83
0.75	0.75	26.90	11.16	1.40	1.07	22.31	11.75	2.38	0.07
0.75	1.00	26.14	11.27	1.49	0.84	22.04	11.75	2.33	0.02
1.00	0.50	26.72	11.23	1.13	1.42	21.00	11.95	2.09	0.00
1.00	0.75	25.75	11.38	1.28	1.00	20.98	11.95	2.08	0.00
1.00	1.00	24.93	11.50	1.42	0.73	20.98	11.95	2.08	0.00
		Zigzag, Dyn.				Zigzag, Sta.			
$c_d$	$c_r$	Revenue	Price	Pickup	Queue	Revenue	Price	Pickup	Queue
0.50	0.50	28.30	10.86	1.36	1.53	27.75	10.97	1.38	1.59
0.50	0.75	27.60	11.00	1.44	1.20	27.16	11.14	1.45	1.32
0.50	1.00	26.87	11.12	1.65	0.88	26.46	11.29	1.62	1.02
0.75	0.50	27.75	11.01	1.26	1.45	27.17	11.13	1.27	1.50
0.75	0.75	26.90	11.16	1.40	1.07	26.40	11.31	1.40	1.16
0.75	1.00	26.14	11.27	1.49	0.84	25.62	11.45	1.48	0.93
1.00	0.50	26.73	11.23	1.15	1.39	26.16	11.35	1.17	1.42
1.00	0.75	25.75	11.38	1.29	0.99	25.23	11.52	1.29	1.06
1.00	1.00	24.93	11.50	1.42	0.73	24.37	11.65	1.41	0.80

**Table 9** Additional performance metrics of different algorithms under parameters  $(L, \Lambda, M) = (20, 8, 10)$ .

2. *Two-radius dispatching, dynamic pricing:* We adopt policy 3 (“Zigzag, Dyn.”) from Section 5.2.2, with modifications to both dispatching and pricing. When using radius-based dispatching, the set of recurrent states may extend beyond the zigzag path, so the original pricing policy does not cover all states. To address this, we set prices for states on the zigzag path using the optimized dynamic prices. For other states, we assign the price from the nearest zigzag-path state with the same driver count  $l$ . Similarly, the thresholds  $r_0$  and  $r_1$  are then selected via a line search over  $\delta$  with step size 0.2 using simulation.

Tables 11 and 12 compare the performance of the two-radius and constant-radius policies. In almost all  $(c_d, c_r)$  settings, the two-radius policies now achieve higher objective values.

## Acknowledgments

The authors thank the support of an Amazon Science Faculty Research Award through the UW-Amazon Science Hub.

		<b>Value Iteration</b>				<b>Greedy, Dyn.</b>			
$c_d$	$c_r$	Revenue	Price	Pickup	Queue	Revenue	Price	Pickup	Queue
0.50	0.50	164.24	9.56	0.41	2.62	160.99	10.25	1.15	1.45
0.50	0.75	164.59	9.59	0.47	2.56	150.34	10.59	1.34	0.73
0.50	1.00	165.01	9.61	0.47	2.54	139.13	11.00	1.33	0.00
0.75	0.50	164.34	9.58	0.38	2.66	160.95	10.25	1.15	1.45
0.75	0.75	164.79	9.59	0.41	2.60	137.48	11.09	1.22	0.00
0.75	1.00	165.08	9.61	0.46	2.54	137.48	11.09	1.22	0.00
1.00	0.50	163.89	9.65	0.34	2.79	134.07	11.24	1.09	0.00
1.00	0.75	164.74	9.60	0.38	2.65	134.07	11.24	1.09	0.00
1.00	1.00	165.23	9.61	0.41	2.58	134.07	11.24	1.09	0.00
		<b>Zigzag, Dyn.</b>				<b>Zigzag, Sta.</b>			
$c_d$	$c_r$	Revenue	Price	Pickup	Queue	Revenue	Price	Pickup	Queue
0.50	0.50	163.11	10.17	0.54	0.71	161.82	10.27	0.52	0.78
0.50	0.75	160.93	10.26	0.58	0.52	159.38	10.38	0.56	0.58
0.50	1.00	159.27	10.32	0.62	0.42	157.49	10.46	0.59	0.47
0.75	0.50	161.13	10.27	0.51	0.62	159.70	10.37	0.50	0.67
0.75	0.75	158.75	10.36	0.55	0.46	157.07	10.47	0.53	0.50
0.75	1.00	157.03	10.43	0.58	0.38	155.13	10.55	0.56	0.41
1.00	0.50	157.30	10.44	0.47	0.52	156.03	10.51	0.47	0.55
1.00	0.75	154.81	10.54	0.51	0.39	153.36	10.62	0.50	0.42
1.00	1.00	152.99	10.60	0.54	0.33	151.38	10.69	0.53	0.35

**Table 10** Additional performance metrics of different algorithms under parameters  $(L, \Lambda, M) = (100, 40, 50)$ .

$c_d$	$c_r$	C.R.		T.R., Sta.		T.R., Dyn.	
		Obj.	Price	Obj.	Price	Obj.	Price
0.50	0.50	114.04	10.68	113.69	10.82	113.85	10.72
0.50	0.80	111.25	10.84	111.37	10.90	111.70	10.79
0.50	1.00	109.45	10.94	109.82	10.97	110.31	10.84
0.80	0.50	90.91	10.84	91.21	10.90	91.28	10.82
0.80	0.80	89.12	10.94	89.40	10.99	89.65	10.89
0.80	1.00	87.85	11.05	88.20	11.05	88.59	10.94
1.00	0.50	69.68	11.05	69.96	11.04	70.00	10.98
1.00	0.80	68.24	11.15	68.58	11.13	68.72	11.06
1.00	1.00	67.47	11.25	67.74	11.19	67.97	11.10

**Table 11** Objective values and average prices under two-radius policies in simulation across various  $(c_d, c_r)$  settings.

$c_d$	$c_r$	C.R.			T.R., Sta.			T.R., Dyn.		
		Revenue	Pickup	Queue	Revenue	Pickup	Queue	Revenue	Pickup	Queue
0.50	0.50	152.12	1.33	0.89	148.58	1.32	0.73	149.23	1.36	0.62
0.50	0.75	147.81	1.43	0.53	145.98	1.38	0.52	146.58	1.44	0.39
0.50	1.00	144.89	1.50	0.36	144.17	1.42	0.41	144.87	1.50	0.28
0.80	0.50	147.92	1.35	0.60	146.09	1.27	0.63	147.15	1.31	0.53
0.80	0.75	144.88	1.33	0.46	143.54	1.32	0.45	144.86	1.36	0.36
0.80	1.00	141.85	1.38	0.30	141.70	1.35	0.35	143.24	1.41	0.26
1.00	0.50	141.88	1.22	0.46	141.95	1.20	0.54	143.08	1.22	0.45
1.00	0.75	138.67	1.27	0.30	139.38	1.24	0.39	140.84	1.26	0.31
1.00	1.00	135.43	1.23	0.25	137.57	1.27	0.30	139.39	1.29	0.24

**Table 12** Additional performance metrics of two-radius policies in terms of revenue rate, average pickup time, and average queueing time in simulation across various  $(c_d, c_r)$  settings.

## Online Appendix

### Appendix EC.1: Proofs

*Proof of Lemma 1.* First, we notice that the sum of the expected number of drivers in service and idle drivers equals the total number of drivers in the system, so we have  $L_o^d(\lambda, \phi) = L - L_s^d(\lambda, \phi)$ . Let  $L_t^d(\lambda, \phi)$  be the expected number of riders on a trip under policy  $(\lambda, \phi)$ . Since the total number of riders in service includes both those waiting to be picked up and those currently on a trip, we have  $L_s^d(\lambda, \phi) = L_p^r(\lambda, \phi) + L_t^d(\lambda, \phi)$ . We consider an observation period  $T$ . Over this period,  $L_t^d(\lambda, \phi)T$  is the total on-trip time for all riders.  $L_t^d(\lambda, \phi)T/t_0$  is the expected number of riders served by the platform over period  $T$ . As  $T \rightarrow \infty$ , by the law of large numbers, the average on-trip time converges to  $t_0$ . Thus, the average number of riders served by the platform per time unit can be computed by  $\lim_{T \rightarrow \infty} L_t^d(\lambda, \phi)T/(t_0T) = L_t^d(\lambda, \phi)/t_0$ . On the other hand, if we increase the base fare  $p_0$  by 1 unit, the objective  $\mathcal{R}(p_0 + 1, \lambda, \phi)$  will increase by the average number of riders served per time unit according to equation (2). Thus, if the platform increases the base fare by  $w_p^r t_0$ , we have  $\mathcal{R}(p_0 + w_p^r t_0, \lambda, \phi) = \mathcal{R}(p_0, \lambda, \phi) + w_p^r t_0 L_t^d(\lambda, \phi)/t_0$ . Consequently, equation (2) can be rewritten as

$$\begin{aligned} & \mathcal{R}(p_0, \lambda, \phi) - w_s^d L_s^d(\lambda, \phi) - w_q^r L_q^r(\lambda, \phi) - w_p^r L_p^r(\lambda, \phi) - w_o^d L_o^d(\lambda, \phi) \\ &= \mathcal{R}(p_0, \lambda, \phi) - w_s^d L_s^d(\lambda, \phi) - w_q^r L_q^r(\lambda, \phi) - w_p^r (L_s^d(\lambda, \phi) - L_t^d(\lambda, \phi)) - w_o^d (L - L_s^d(\lambda, \phi)) \\ &= \mathcal{R}(p_0, \lambda, \phi) + \frac{w_p^r t_0 L_t^d(\lambda, \phi)}{t_0} - (w_s^d + w_p^r - w_o^d) L_s^d(\lambda, \phi) - w_q^r L_q^r(\lambda, \phi) - w_o^d L \\ &= \mathcal{R}(p_0 + w_p^r t_0, \lambda, \phi) - (w_s^d + w_p^r - w_o^d) L_s^d(\lambda, \phi) - w_q^r L_q^r(\lambda, \phi) - w_o^d L, \end{aligned}$$

which proves the result.  $\square$

*Proof of Lemma 2.* We start with the proof of condition (1). Let  $(l', m')$  be a type 1 state. To show that  $(l, m)$  is also a type 1 state for any  $l' \leq l \leq L - 1$  and  $1 \leq m \leq m'$ , it is sufficient to show that  $(l' + 1, m')$  and  $(l', m' - 1)$  are both type 1 state. Then condition (1) can be proved by recursively applying this result. We first show that  $(l' + 1, m')$  is a type 1 state. According to Assumption 1, we have

$$(l' + 1)\mu_{l'+1, m'} - (l' + 1)\mu_{l'+1, m'-1} \geq l'\mu_{l', m'} - l'\mu_{l', m'-1}, \quad (\text{EC.1})$$

$$(l' + 1)\mu_{l'+1, m'-1} - (l' + 2)\mu_{l'+2, m'-1} \geq l'\mu_{l', m'-1} - (l' + 1)\mu_{l'+1, m'-1}. \quad (\text{EC.2})$$

Inequality (EC.1) is from condition (1) in Assumption 1, and inequality (EC.2) is from condition (2) in Assumption 1. Summing equation (EC.1) with equation (EC.2) on both sides yields

$$(l' + 1)\mu_{l'+1, m'} - (l' + 2)\mu_{l'+2, m'-1} \geq l'\mu_{l', m'} - (l' + 1)\mu_{l'+1, m'-1} > 0, \quad (\text{EC.3})$$

where the second inequality is due to the fact that  $(l', m')$  is a type 1 state which satisfies  $l'\mu_{l', m'} > (l' + 1)\mu_{l'+1, m'-1}$ . Equation (EC.3) yields  $(l' + 1)\mu_{l'+1, m'} > (l' + 2)\mu_{l'+2, m'-1}$ , which shows that  $(l' + 1, m')$  is a type 1 state by definition. To show  $(l', m' - 1)$  is also a type 1 state, similarly, Assumption 1 gives

$$l'\mu_{l', m'-1} - l'\mu_{l', m'-2} \geq l'\mu_{l', m'} - l'\mu_{l', m'-1}, \quad (\text{EC.4})$$

$$l'\mu_{l', m'-2} - (l' + 1)\mu_{l'+1, m'-2} \geq l'\mu_{l', m'-1} - (l' + 1)\mu_{l'+1, m'-1}. \quad (\text{EC.5})$$

Summing equation (EC.4) with equation (EC.5) on both sides, we get

$$l'\mu_{l', m'-1} - (l' + 1)\mu_{l'+1, m'-2} \geq l'\mu_{l', m'} - (l' + 1)\mu_{l'+1, m'-1} > 0,$$

which shows that  $(l', m' - 1)$  is a type 1 state.

So far, we have proved condition (1). Now we consider the case when  $(l', m')$  is a type 2 state. If there exists some type 1 state  $(l_1, m_1)$  such that  $l_1 \leq l'$  and  $m_1 \geq m'$ , according to condition 1, we know  $(l', m')$  must be a type 1 state as well, which leads to contradiction. Hence, we know condition (2) holds.  $\square$

*Proof of Theorem 1.* We prove the theorem under three cases  $c_d = c_r$ ,  $c_d > c_r$ , and  $c_d < c_r$ .

**Case 1:  $c_d = c_r$ .** Let  $\phi^*$  be the optimal dispatching policy such that  $\phi^*(l, m) = 0$  for all type 1 states and  $\phi^*(l, m) = 1$  for all type 2 states and  $\lambda^*$  the optimal dynamic pricing policy. We want to show  $\tilde{\mathcal{R}}(\lambda^*, \phi^*) \geq \tilde{\mathcal{R}}(\phi, \lambda)$  for an arbitrary policy  $(\phi, \lambda)$ . We consider a coupling of two systems, where system 1 uses the optimal dispatching policy and system 2 uses the policy  $(\phi, \lambda)$ . This coupling aligns all random events in both systems, including arrivals, trip completions, and dispatches. Instead of using the optimal pricing policy  $\lambda^*$  for system 1, we apply a dependent pricing policy  $\lambda^D$  that is dependent on system 2. Specifically,  $\lambda^D$  is constructed to keep the effective request rate in system 1 always the same as that in system 2, even if the two systems are in different states. In other words, for any state transition in system 2, the effective request rate in system 1 is immediately adjusted to the same as the new effective request rate in system 2. We know  $\tilde{\mathcal{R}}(\phi^*, \lambda^*) \geq \tilde{\mathcal{R}}(\phi^*, \lambda^D)$ . Thus, it is sufficient to show  $\tilde{\mathcal{R}}(\phi^*, \lambda^D) \geq \tilde{\mathcal{R}}(\phi, \lambda)$ . We demonstrate this in the following.

Let  $\{X_t\}_{t=1}^\infty$  and  $\{Y_t\}_{t=1}^\infty$  denote the coupled Markov chain, where each step  $t$  corresponds to a transition in the joint process. At step  $t$ , the state of system 1 is given by  $X_t = (l_t, m_t)$ , and the state of system 2 is given by  $Y_t = (l'_t, m'_t)$ . Without loss of generality, we assume that both systems start with the same number of busy drivers and riders in the queue, that is,  $X_1 = Y_1$ . If a random event occurs in either system at step  $t$ , the states of systems 1 and 2 transition to  $X_{t+1}$  and  $Y_{t+1}$  after possible dispatchings, respectively, based on their dispatching policies. After that, the coupled chain proceeds to step  $t+1$ . In the following, we show that under coupling, there are three possible “phases”, which are mutually exclusive, for the pair  $(X_t, Y_t)$  at step  $t$ . The coupled process loops over these phases. Moreover, at each phase, the two systems have identical revenue rates, while the penalty rate in system 1 is consistently less than or equal to one in system 2.

**Phase 1.** At step  $t$ , the process is in phase 1 if  $X_t = Y_t = (l_t, m_t)$ . Since both systems are in the same state and the effective request rate in system 1 is always set to be the same as that in system 2, there are two possible events for the coupled systems: (1) a rider joining the queue for both systems; (2) a trip completion for both systems. In both cases, if the number of dispatched drivers under  $\phi^*$  and  $\phi$  is the same, then  $X_{t+1} = Y_{t+1}$ , and the process remains in phase 1. Otherwise, if the two policies dispatch a different number of drivers, the coupled states  $X_{t+1} \neq Y_{t+1}$ . Since the system will lie in the same anti-diagonal after dispatching, we know both systems lie in the same anti-diagonal at step  $t+1$  under each event. Then, the process leaves phase 1 and enters phase 2 at step  $t+1$ .

**Phase 2.** At step  $t$ , the process is in phase 2 if  $X_t = (l_t, m_t) \neq Y_t = (l'_t, m'_t)$  and  $l_t + m_t = l'_t + m'_t$  (i.e.,  $X_t$  and  $Y_t$  are on the same anti-diagonal line). By Lemma 2, the total service rate follows  $l_t \mu_{l_t, m_t} \geq l'_t \mu_{l'_t, m'_t}$ . We can decompose the rate  $l_t \mu_{l_t, m_t}$  in system 1 into two portions,  $l'_t \mu_{l'_t, m'_t}$  and  $l_t \mu_{l_t, m_t} - l'_t \mu_{l'_t, m'_t}$ , where we couple the first portion with system 2 and leave the second portion as uncoupled. Thus, there are three possible events for the coupled systems: (1) a rider joining the queue for both systems; (2) a trip completion for both systems; (3) a trip completion only for system 1 (due to the second portion). For events (1) and (2), as the number of dispatched drivers does not affect the sum of  $l_{t+1}$  and  $m_{t+1}$ , both systems will lie on the same anti-diagonal line at step  $t+1$ . If  $X_{t+1} \neq Y_{t+1}$ , the process stays at phase 2. If  $X_{t+1} = Y_{t+1}$ , the process leaves phase 2 and re-enters phase 1. For event (3), we have  $l_{t+1} + m_{t+1} < l'_{t+1} + m'_{t+1}$ , and the process leaves phase 2 and enters into phase 3.

**Phase 3.** At step  $t$ , the process is in phase 3 if  $l_t + m_t < l'_t + m'_t$ . In this phase, we cannot determine which state,  $X_t$  or  $Y_t$ , has the higher total service rate. Thus, there are four possible events for the coupled systems: (1) a rider joining the queue for both systems; (2) a trip completion for both systems; (3) a trip completion only for system 1; (4) a trip completion only for system 2. For events (1), (2), and (3), the process stays at phase 3 since one can easily show that  $l_{t+1} + m_{t+1} < l'_{t+1} + m'_{t+1}$  holds. For events (4), there are two possible sub-cases:  $l'_{t+1} + m'_{t+1} = l_{t+1} + m_{t+1}$  and  $l'_{t+1} + m'_{t+1} > l_{t+1} + m_{t+1}$ . If  $l'_{t+1} + m'_{t+1} = l_{t+1} + m_{t+1}$ , then the process leaves phase 3 and re-enters either phase 1 (when  $X_{t+1} = Y_{t+1}$ ) or phase 2 (when  $X_{t+1} \neq Y_{t+1}$ ). Otherwise, if  $l'_{t+1} + m'_{t+1} > l_{t+1} + m_{t+1}$ , the process stays at phase 3.

In all phases, since the effective request rate for both systems are kept the same, the revenue rate for both systems are the same as well. However, under coupling, the penalty rate in system 1 is consistently less or equal to that in system 2 because of weakly smaller  $l+m$  values. Hence, we have  $\tilde{\mathcal{R}}(\phi^*, \lambda^*) \geq \tilde{\mathcal{R}}(\phi^*, \lambda^D) \geq \tilde{\mathcal{R}}(\phi, \lambda)$ , which proves the result. The first inequality holds because there always exists an optimal Markovian policy (see Theorem 8.1.2 of Puterman 2014).

**Case 2:  $c_d > c_r$ .** We show that there exists a policy  $(\phi^D, \lambda^D)$  such that  $\tilde{\mathcal{R}}(\phi^D, \lambda^D) \geq \tilde{\mathcal{R}}(\phi, \lambda)$  holds for any policy  $(\phi, \lambda)$ . Construct  $\phi^D$  such that  $\phi^D(l, m) = 0$  for all type 1 states  $(l, m)$ . We consider a coupling of two

systems, where system 1 uses policy  $(\phi^D, \lambda^D)$  and system 2 uses policy  $(\phi, \lambda)$ . Similar to the case of  $c_d = c_r$ ,  $\lambda^D$  here is defined to keep the effective request rate in system 1 always the same as that in system 2. Again, let  $\{X_t\}_{t=1}^\infty$  and  $\{Y_t\}_{t=1}^\infty$  denote the coupled Markov chain, where each step  $t$  corresponds to a transition in the joint process. In the following, we describe the coupling processes and the constructed dispatching policy  $\phi^D$  in each phase.

**Phase 1.** At step  $t$ , the process is in phase 1 if  $X_t = Y_t$ . Let  $X_t = (l_t, m_t)$  denote the corresponding state of system 1 at step  $t$ . There are two possible events for the coupled systems, which are the same as those in case  $c_d = c_r$ , phase 1. Under this phase, we set  $\phi^D(l, m) = \phi(l, m)$ , which is the dispatching policy in system 2, for all type 2 states  $(l, m)$ . We now consider next state  $Y_{t+1} = (l'_{t+1}, m'_{t+1})$  for system 2. Let  $P^*$  be the corresponding zigzag path under  $\phi^*$ , the optimal dispatching policy when  $c_d = c_r$ . If  $Y_{t+1}$  is a type 2 state or  $Y_{t+1} \in P^*$ , then by the construction of  $\phi^D$ , both systems dispatch the same number of drivers at step  $t$ , so we have  $X_{t+1} = Y_{t+1}$ . The process remains in phase 1. Otherwise, if  $Y_{t+1}$  is a type 1 state and  $Y_{t+1} \notin P^*$ , then the number of dispatched drivers differs between the two policies, so we have  $X_{t+1} \neq Y_{t+1}$ . Since  $\phi^D(l, m) = 0$  for all type 1 states  $(l, m)$ , we know  $X_{t+1} \in P^*$ . Moreover,  $X_{t+1}$  and  $Y_{t+1}$  still lie on the same anti-diagonal, and  $l_{t+1} < l'_{t+1}$ . The process leaves phase 1 and enters into phase 2.

**Phase 2.** At step  $t$ , the process is in phase 2 if  $l_t < l'_t$ ,  $m_t > m'_t$ ,  $l_t + m_t = l'_t + m'_t$ , and  $X_t \in P^*$ . In other words,  $Y_t$  lies on the same anti-diagonal as  $X_t$  but is positioned to the lower left of  $X_t$ . In this phase, we set  $\phi^D = \phi^*$ , which is the optimal dispatching policy when  $c_d = c_r$ . The coupled systems face the same three events defined in phase 2, case 1 ( $c_d = c_r$ ). Again, we use the same label (1), (2), and (3) described in phase 2, case 1 to represent each event. When event (1) or (2) occurs, if  $X_{t+1} \neq Y_{t+1}$ , we know  $l_{t+1} < l'_{t+1}$  as  $\phi^*$  makes at most one dispatch after an event occurs. Thus, the process stays at phase 2. If  $X_{t+1} = Y_{t+1}$ , the process leaves phase 2 and re-enters into phase 1. When event (3) occurs, we have  $l_{t+1} < l'_{t+1}$  and  $l_{t+1} + m_{t+1} < l'_{t+1} + m'_{t+1}$ , and the process leaves phase 2 and enters phase 3.

**Phase 3.** At step  $t$ , the process is in phase 3 if  $l_t < l'_t$  and  $l_t + m_t < l'_t + m'_t$ . There are four possible events for the coupled systems, which are exactly the same as those in phase 3, case 1. Now we use event (1), (2), (3), and (4) to describe each event. We set dispatching policy  $\phi^D$  to be dependent on the event that occurred. If event (1), (2), or (3) occurs next, the two systems keep their anti-diagonal relationship, that is,  $l_{t+1} + m_{t+1} < l'_{t+1} + m'_{t+1}$ . Under these events, we set  $\phi^D(l, m) = 0$  for all type 2 states  $(l, m)$ , which means system 1 will not make a dispatch under these events. Moreover, for event (1), we have  $m_{t+1} = m_t + 1 > m'_t + 1 \geq m'_{t+1}$  and  $l_{t+1} = l_t < l'_t \leq l'_{t+1}$ . For events (2) and (3), we have  $m_{t+1} = m_t > m'_t \geq m'_{t+1}$  and  $l_{t+1} = l_t - 1 < l'_t - 1 \leq l'_{t+1}$ . Thus, the process will stay at phase 3 since all conditions for phase 3 are satisfied.

For event (4), we have  $l_{t+1} + m_{t+1} = l_t + m_t$  and  $l'_{t+1} + m'_{t+1} = l'_t + m'_t - 1$ . If  $l_{t+1} + m_{t+1} < l'_{t+1} + m'_{t+1}$ , we set  $\phi^D(l, m) = 0$  for all type 2 states  $(l, m)$  as well. Then we know  $m_{t+1} = m_t > m'_t \geq m'_{t+1}$ , and thus  $l_{t+1} < l'_{t+1}$  holds. As a result, the process will stay at phase 3. Otherwise, if  $l_t + m_t = l'_{t+1} + m'_{t+1}$ , we set  $\phi^D = \phi^*$ , the optimal dispatching policy when  $c_d = c_r$ . It is easy to verify that the process will enter phase 1 if  $l_{t+1} = l'_{t+1}$  or phase 2 if  $l_{t+1} < l'_{t+1}$ .

In all phases, the revenue rate is identical for both systems, while the penalty rate in system 1 is always less than or equal to that in system 2 at coupled states because system 1 has weakly smaller  $l + m$  and  $l$  values. Hence, again the objective function satisfies  $\tilde{\mathcal{R}}(\phi^*, \lambda^*) \geq \tilde{\mathcal{R}}(\phi^D, \lambda^D) \geq \tilde{\mathcal{R}}(\phi, \lambda)$ , which proves the result.

**Case 3:**  $c_d < c_r$ . Similar to case 2, we show there exists  $\phi^D$  and  $\lambda^D$  such that  $\tilde{\mathcal{R}}(\phi^D, \lambda^D) \geq \tilde{\mathcal{R}}(\phi, \lambda)$  for an arbitrary policy  $(\phi, \lambda)$ . We set  $\lambda^D$  to keep the effective request rate in system 1 always the same as that in system 2. We set  $\phi^D$  such that  $\phi^D(l, m) = 1$  for all type 2 states  $(l, m)$ . For type 1 states,  $\phi^D$  depends on system 2, and will be defined later. Again, let  $\{X_t\}_{t=1}^\infty$  and  $\{Y_t\}_{t=1}^\infty$  denote the coupled Markov chain, where each step  $t$  corresponds to a transition in the joint process. There are four possible phases in this case, which are illustrated below.

**Phase 1.** At step  $t$ , the process is in phase 1 if  $X_t = Y_t$ . Under this phase, if  $Y_{t+1}$  is a type 1 state, we set  $\phi^D = \phi$  for all type 1 states. Then the next coupled states satisfy  $X_{t+1} = Y_{t+1}$ , and the process remains in phase 1. Otherwise, if  $Y_{t+1}$  is a type 2 state, we set  $\phi^D = 0$  for all type 1 states (i.e.,  $\phi^D = \phi^*$ ). The next coupled states satisfy  $X_{t+1} \neq Y_{t+1}$  and  $X_{t+1} \in P^*$  since  $\phi^D(l, m) = 1$  for all type 2 states. Since the state will always stay on the same anti-diagonal after a dispatching action, we have  $l_{t+1} + m_{t+1} = l'_{t+1} + m'_{t+1}$  and  $m_{t+1} < m'_{t+1}$ . The process leaves phase 1 and enters phase 2.

**Phase 2.** At step  $t$ , the process is in phase 2 if  $m_t < m'_t$ ,  $l_t > l'_t$ ,  $l_t + m_t = l'_t + m'_t$ ,  $X_t \in P^*$ , and thus,  $Y_t$  is a type 2 state. There are three possible events for the coupled systems, which are the same as those in

phase 2, case 1. If  $Y_{t+1}$  is a type 2 state, we set  $\phi^D = \phi^*$ , the optimal dispatching policy under  $c_d = c_r$ . Then  $X_{t+1} \in P^*$  is a type 1 state. When event (1) or (2) occurs, we have  $l_{t+1} + m_{t+1} = l'_{t+1} + m'_{t+1}$ . Since  $Y_{t+1}$  is a type 2 state, we know  $m_{t+1} < m'_t$  and  $l_{t+1} > l'_{t+1}$  hold. Thus, the process stays in phase 2. When event (3) occurs, we have  $l_{t+1} + m_{t+1} = l_t + m_t - 1 < l'_t + m'_t = l'_{t+1} + m'_{t+1}$ . Moreover,  $m_{t+1}$  either equals to  $m_t$  (not dispatch) or  $m_t - 1$  (dispatch), which is strictly less than  $m'_t$ . The process then enters phase 3.

Otherwise, if  $Y_{t+1}$  is a type 1 state, we set  $\phi^D = \phi$ . Only event (1) or (2) can occur because  $Y_t$  is a type 2 state, so there must be a state transition in system 2. Thus, we have  $l_{t+1} + m_{t+1} = l'_{t+1} + m'_{t+1}$ . Moreover, we know  $X_{t+1} = Y_{t+1}$  because both systems have the same dispatching policy at type 1 states and  $Y_{t+1}$  becomes a type 1 state now. Consequently, the process leaves phase 2 and enters phase 1 again.

**Phase 3.** At step  $t$ , the process is in phase 3 if  $m_t < m'_t$ ,  $l_t + m_t < l'_t + m'_t$ , and  $X_t \in P^*$ . There are four possible events for the coupled systems, which are exactly the same as those in phase 3, case 1. We construct  $\phi^D$  according to  $m'_{t+1}$ . If  $m_t > m'_{t+1}$ , at all type 1 states, we set  $\phi^D$  to keep dispatching until  $m_{t+1} = m'_{t+1}$ . Note that event (3) is not possible to occur under  $m_t > m'_{t+1}$ . In specific, we set  $\phi^D$  under events (1), (2), and (4) according to the following:

- (a) Under event (1), for every  $k = 0, \dots, \min\{L - l_t, m_t - m'_{t+1} + 1\}$ , we set  $\phi^D(l_t + k, m_t + 1 - k) = 1$ ;
- (b) Under event (2), for every  $k = 0, \dots, \min\{L - l_t + 1, m_t - m'_{t+1}\}$ , we set  $\phi^D(l_t - 1 + k, m_t - k) = 1$ ;
- (c) Under event (4), for every  $k = 0, \dots, \min\{L - l_t, m_t - m'_{t+1}\}$ , we set  $\phi^D(l_t - 1 + k, m_t - k) = 1$ .

For any type 1 state not covered above, we set  $\phi^D(l, m) = 0$ . On the other hand, if  $m_t \leq m'_{t+1}$ , we set  $\phi^D = \phi^*$ , the optimal dispatching policy under  $c_d = c_r$ . In the following, we discuss what happens for systems 1 and 2 under each event.

For events (1) and (2), if  $m_t > m'_{t+1}$  due to dispatching in system 2, we make dispatches in system 1 to state  $m_{t+1} = m'_{t+1}$ . Since both systems have an arrival or a trip completion, we have  $l_{t+1} + m_{t+1} < l'_{t+1} + m'_{t+1}$ . Then, the process enters into phase 4. If  $m_t \leq m'_{t+1}$ , we have  $\phi^D = \phi^*$ , so we know  $X_{t+1} \in P^*$  and  $l_{t+1} + m_{t+1} < l'_{t+1} + m'_{t+1}$ . We have two sub-cases here. If  $m_{t+1} = m'_{t+1}$ , the process enters phase 4. Otherwise, if  $m_{t+1} < m'_{t+1}$ , the process stays in phase 3.

For event (3), the state  $Y_{t+1}$  is the same as  $Y_t$ , so we have  $m_t < m'_t = m'_{t+1}$ . As a result,  $\phi^D$  is set as  $\phi^*$ . Consequently,  $m_{t+1} \leq m_t < m'_t = m'_{t+1}$  and  $X_{t+1} \in P^*$  hold. The process stays at phase 3.

For event (4), there are two sub-cases: (a)  $l_t + m_t = l'_{t+1} + m'_{t+1}$ , that is, the two systems are on the same anti-diagonal. Since  $m_{t+1} \leq m_t$  holds, we know  $m_{t+1} \leq m'_{t+1}$  holds according to our constructed  $\phi^D$ . If  $m'_{t+1} = m_{t+1}$ , the process re-enters phase 1. If  $m_{t+1} < m'_{t+1}$ , we know  $\phi^D$  is constructed as  $\phi^*$ . Thus, the process re-enters phase 2. (b)  $l_t + m_t < l'_{t+1} + m'_{t+1}$ . If  $m_t < m'_{t+1}$ , we set  $\phi^D = \phi^*$ , so the state in system 1 does not change (i.e.,  $l_{t+1} = l_t$  and  $m_{t+1} = m_t$ ). Thus, the process stays at phase 3. If  $m_t > m'_{t+1}$ , according to constructed  $\phi^D$ , we have  $m_{t+1} = m'_{t+1}$ . The process enters phase 4. If  $m_t = m'_{t+1}$ , we set  $\phi^D = \phi^*$ , and the process also enters phase 4 due to  $m_{t+1} = m_t = m'_{t+1}$ .

**Phase 4.** At step  $t$ , the process is in phase 4 if  $m_t = m'_t$ ,  $l_t < l'_t$ , and  $l_t + m_t < l'_t + m'_t$  hold. There are four possible events for the coupled system, which are exactly the same as those in phase 3, case 1. We construct  $\phi^D$  according to the state type of  $Y_{t+1}$ . If  $Y_{t+1}$  is a type 1 state, we use the same construction of  $\phi^D$  as one in phase 3 under  $m_t > m'_{t+1}$ . That is, at all type 1 states,  $\phi^D$  is set to keep dispatching until  $m_{t+1} \leq m'_{t+1}$  (i.e., dispatching the same number of drivers in both systems if system 1 is still in a type 1 state before taking the action). Otherwise, if  $Y_{t+1}$  is a type 2 state, we set  $\phi^D = \phi^*$ .

For events (1) and (2), if  $Y_{t+1}$  is a type 1 state, we have two subcases: (a)  $(l_t - 1, m_t)$  is a type 1 state under event (1) or  $(l_t, m_t + 1)$  is a type 1 state under event (2). In this case, both systems dispatch the same number of drivers. Thus, we have  $m_{t+1} = m'_{t+1}$  and the process stays in phase 4. (b)  $(l_t - 1, m_t)$  is a type 2 state under event (1) or  $(l_t, m_t + 1)$  is a type 2 state under event (2). If system 2 dispatches at least one driver, then according to the construction of  $\phi^D$ , both systems dispatch the same number of drivers as well, so the process stays in phase 4. If system 2 does not dispatch any drivers, system 1 will dispatch exactly one driver since we require  $\phi^D(l, m) = 1$  for all type 2 states. Therefore, it follows  $m_{t+1} = m_t - 1 = m'_t - 1 = m'_{t+1} - 1 < m'_{t+1}$  and  $X_{t+1} \in P^*$  after dispatching, so the process enters phase 3.

Otherwise, if  $Y_{t+1}$  is a type 2 state, we know there is no dispatching in system 2 at step  $t$  since  $Y_t$  is a type 1 state. By zigzag property, we know both  $(l_t - 1, m_t)$  and  $(l_t, m_t + 1)$  are type 2 states, so system 1 will make a dispatch. Then we have  $m_{t+1} < m'_{t+1}$ , and  $X_{t+1} \in P^*$ . Thus, the process re-enters phase 3.

For event (3),  $Y_{t+1}$  is the same as  $Y_t$ , so we have  $m'_{t+1} = m'_t = m_t$ . If  $(l_t - 1, m_t)$  is a type 1 state, we have  $m_{t+1} = m_t = m'_t = m'_{t+1}$ , so the process stays at phase 4. On the other hand, if  $(l_t - 1, m_t)$  is a type 2

state, system 1 will make a dispatch and go into a type 1 state. Thus, we have  $m_{t+1} < m_t = m'_t = m'_{t+1}$  and  $X_{t+1} \in P^*$ , so the process re-enters phase 3.

For event (4),  $Y_{t+1}$  must be a type 1 state. This is because  $X_t = (l_t, m_t)$  is a type 1 state, and  $l_t \leq l'_{t+1}$  and  $m_t \geq m'_{t+1}$  hold, so by Lemma 2,  $Y_{t+1} = (l'_{t+1}, m'_{t+1})$  is also a type 1 state. Then, according to the construction of  $\phi^D$ , we have  $m_{t+1} = m'_{t+1}$  since the number of dispatches under the event is the same in both system 1 and system 2. Thus, if  $l_t + m_t < l'_{t+1} + m'_{t+1}$  holds, the process stays at phase 4. Otherwise, if  $l_t + m_t = l'_{t+1} + m'_{t+1}$ , the next states  $X_{t+1} = Y_{t+1}$ , so the process returns to phase 1.

In all phases, the revenue rate is identical for both systems, while the penalty rate in system 1 is always less than or equal to that in system 2 at coupled states because system 1 has weakly smaller  $l + m$  and  $m$  values. Hence, again the objective function satisfies  $\bar{\mathcal{R}}(\phi^*, \lambda^*) \geq \bar{\mathcal{R}}(\phi^D, \lambda^D) \geq \bar{\mathcal{R}}(\phi, \lambda)$ , which proves the result.  $\square$

*Proof of Theorem 2.* By Theorem 1, when  $c_d = c_r$ , there exists an optimal dispatching policy  $\phi^*$  that satisfies  $\phi^*(l, m) = 0$  for all type 1 states and  $\phi^*(l, m) = 1$  for all type 2 states. Let  $P^* = ((l_1, m_1), (l_2, m_2), \dots)$  be the corresponding zigzag path under  $\phi^*$  and  $P_j^* := ((l_1, m_1), \dots, (l_j, m_j))$  be a sub-path of  $P^*$  that terminates at state  $(l_j, m_j) \in P^*$ . In the following, we show that when  $c_d = c_r$ ,  $P_j^*$  yields an objective based on optimal static pricing that is greater than or equal to any other zigzag paths terminating at state  $(l_j, m_j)$  when we compare two paths in Algorithm 1 (i.e.,  $P_{l_j, m_j} = P_j^*$  for  $j = 1, 2, \dots$ , where  $P_{l, m}$  stores the best zigzag path terminated at  $(l, m)$  when Algorithm 1 terminates).

We use induction to show this. Recall that in Algorithm 1, we evaluate the objective values of the two predecessor paths leading into state  $(l_j, m_j)$ : one arriving from above and the other from the left. For  $k = 1, 2, \dots$ , suppose that path  $P_k^*$  follows  $P_{l_k, m_k} = P_k^*$ . This holds trivially for  $k = 1$ . We want to show  $P_{l_{k+1}, m_{k+1}} = P_{k+1}^*$  holds as well. We have the following two cases.

- (1)  $l_{k+1} = l_k$  and  $m_{k+1} = m_k + 1$ , that is,  $P_{\text{left}} = P_{k+1}^*$  when Algorithm 1 is at  $(l_{k+1}, m_{k+1})$ . We show that  $\mathcal{R}_{\text{left}} \geq \mathcal{R}_{\text{above}}$ . Similar to the proof idea of Theorem 1, we construct a coupling between two systems: system 1 follows path  $P_{\text{left}}$  and system 2 follows  $P_{\text{above}}$ . Both systems adopt the same static pricing, and we align their cutoff states so that the cutoff state in system 1 lies on the same anti-diagonal (same  $l + m$  value) as the cutoff state in system 2. Under this coupling, the revenue rates are identical when neither system is at its cutoff state. Moreover, for states at the same anti-diagonal, the total service rate in system 1 is greater than or equal to that in system 2, so its penalty rate is always no greater than that of system 2 under coupling. In addition, system 1 never reaches its cutoff state if system 2 is not at its cutoff state. Together, these facts imply that the objective of system 1 is at least as large as that of system 2, i.e.,  $\mathcal{R}_{\text{left}} \geq \mathcal{R}_{\text{above}}$ . If the objectives under the two paths satisfy  $\mathcal{R}_{\text{left}} > \mathcal{R}_{\text{above}}$ , according to Algorithm 1, we have  $P_{l_{k+1}, m_{k+1}} = P_{k+1}^*$ . Otherwise, if we have  $\mathcal{R}_{\text{left}} = \mathcal{R}_{\text{above}}$ , since  $(l_{k+1} - 1, m_{k+1})$  must be a type 2 state as it is not on the optimal zigzag path  $P^*$ , according to Algorithm 1, we have  $P_{l_{k+1}, m_{k+1}} = P_{k+1}^*$  as well.
- (2)  $l_{k+1} = l_k + 1$  and  $m_{k+1} = m_k$ , that is,  $P_{\text{above}} = P_{k+1}^*$ . Under a similar coupling argument, one can show that  $\mathcal{R}_{\text{above}} \geq \mathcal{R}_{\text{left}}$ . If the objectives satisfy  $\mathcal{R}_{\text{above}} > \mathcal{R}_{\text{left}}$ , we have  $P_{l_{k+1}, m_{k+1}} = P_{k+1}^*$ . If the objectives satisfy  $\mathcal{R}_{\text{left}} = \mathcal{R}_{\text{above}}$ , then  $(l_{k+1} - 1, m_{k+1})$  must be a type 1 state. Thus, according to Algorithm 1, we have  $P_{k+1}^* = P_{l_{k+1}, m_{k+1}}$ .

Therefore, by induction, Algorithm 1 will set  $P_{l_j, m_j} = P^*$  for every  $j = 1, 2, \dots$ . Thus, Algorithm 1 yields the same optimal dispatching policy described in Theorem 1. Moreover, the corresponding pricing policy  $\lambda^*$  converges to the optimal solution under value iteration, so the pricing policy is optimal as well.  $\square$

*Proof of Proposition 1.* Consider the threshold  $M \geq L\bar{\mu}p_{\max}/c_r$ . First, we notice that for any  $l \in \mathcal{L}$  and any  $m \geq M$ , we have

$$p_{\max} \leq \frac{c_d l + c_r m}{l\mu_{l, m}}. \quad (\text{EC.6})$$

To see why, we start with the chosen threshold condition:

$$M \geq \frac{L\bar{\mu}p_{\max}}{c_r} \implies \frac{c_r M}{L\bar{\mu}} \geq p_{\max}. \quad (\text{EC.7})$$

Since  $m \geq M$  and  $\bar{\mu} \geq \mu_{l, m} > 0$ , we have

$$\frac{c_d l + c_r m}{l\mu_{l, m}} \geq \frac{c_r M}{l\bar{\mu}} \geq \frac{c_r M}{L\bar{\mu}} \geq p_{\max} \quad (\text{EC.8})$$

for any  $l \leq L$ . Now, consider extending the path  $P = ((l_1, m_1), \dots, (l_I, m_I))$  to some state  $(l_{I+1}, m_{I+1})$  where  $m_{I+1} \geq M$ . Let the extended path be  $P' := ((l_1, m_1), \dots, (l_{I+1}, m_{I+1}))$ . We show that the objective under the optimal dynamic pricing for  $P'$  is the same as that for path  $P$ . To illustrate this, we examine a cycle of recurrence of the process that starts and ends at  $(l_I, m_I)$ . Within this cycle, if the first event is a trip completion, then the expected return in this cycle will be the same as that of the original path  $P$  starting at  $(l_I, m_I)$ . On the other hand, if the first event is an effective arrival, the state transitions to  $(l_{I+1}, m_{I+1})$ . Then the expected time for the Markov chain to return to state  $(l_I, m_I)$  is  $1/(l_{I+1}\mu_{l_{I+1}, m_{I+1}})$ . During this period, the expected accumulated penalty is  $(c_d l_{I+1} + c_r m_{I+1})/(l_{I+1}\mu_{l_{I+1}, m_{I+1}})$ . However, the revenue coming from a single arrival is at most  $p_{\max}$ , which is less than or equal to the penalty by equation (EC.6). Thus optimal dynamic pricing on  $P'$  will not admit any new rider arrival at state  $(l_I, m_I)$ .

Clearly, the same argument works for optimal static pricing under path comparison in Algorithm 1: when  $m > M$ , extending the path from state  $(l-1, m)$  or  $(l, m-1)$  to state  $(l, m)$  will not improve the objective under any static pricing. Therefore, for  $m > M$  and  $l \in \mathcal{L}$ , the objective recorded at each state  $R_{l,m}$  satisfies  $R_{l,m} = \max\{R_{l,m-1}, R_{l-1,m}\}$ . As a consequence, for  $m > M$ , the following equation holds:

$$\begin{aligned} R_{L,m} &= \max\{R_{L,m-1}, R_{L-1,m}\} \\ &= \max\{R_{L,m-1}, R_{L-1,m-1}, R_{L-2,m}\} \\ &= \max\{R_{L,m-1}, R_{L-1,m-1}, \dots, R_{1,m}\} \\ &= \max_{l \in \{1, \dots, L\}} \{R_{l,m-1}\} \\ &= \max_{l \in \{1, \dots, L\}} \{R_{l,M}\} = R_{L,M}. \end{aligned}$$

Thus, extending a path to any state  $(l, m), m > M$  cannot produce a better solution. This completes the proof.  $\square$

*Proof of Proposition 2.* Given the estimated parameters  $\hat{\alpha}_2, \hat{\alpha}_2$  and  $\hat{C}$ , the predicted service rate at state  $(l, m)$  can be written as

$$\hat{\mu}_{l,m} = \frac{1}{\hat{C}(m+1)^{\hat{\alpha}_1}(L-l+1)^{\hat{\alpha}_2} + t_0}.$$

Since the fitted coefficient  $\hat{\alpha}_1, \hat{\alpha}_2 < 0$ , we know  $\hat{\mu}_{l,m}$  is strictly increasing in  $m$  and strictly decreasing in  $l$ . To verify Assumption 1, we need to show that the differences in the total service rate,  $l\mu_{l,m+1} - l\mu_{l,m}$  and  $l\mu_{l,m} - (l+1)\mu_{l+1,m}$ , are both non-increasing in  $m$  and non-decreasing in  $l$ . Instead of directly proving this, we establish a stronger result: the partial differences  $\mu_{l,m+1} - \mu_{l,m}$  and  $\mu_{l,m} - \mu_{l+1,m}$  are non-increasing in  $m$  and non-decreasing in  $l$ . We first perform a variable transformation on  $l$  by replacing it with  $o = L - l$ , where  $o$  represents the number of idle drivers. Under this transformation, with a bit abuse of notation, we denote the service rate as  $\hat{\mu}(o, m)$ . We further extend the domain of  $o$  and  $m$  to continuous values, with  $o \in [0, L]$  and  $m \in [0, +\infty]$ . In specific,  $\hat{\mu}(o, m)$  can be written as

$$\hat{\mu}(o, m) = \frac{1}{\hat{C}(m+1)^{\hat{\alpha}_1}(o+1)^{\hat{\alpha}_2} + t_0}.$$

Since  $\hat{\mu}(o, m)$  is continuously differentiable, it suffices to show that its Hessian matrix is element-wise non-positive. More specifically, we need to confirm that:

$$\frac{\partial^2 \hat{\mu}}{\partial o \partial m} \leq 0, \quad \frac{\partial^2 \hat{\mu}}{\partial^2 o} \leq 0, \quad \text{and} \quad \frac{\partial^2 \hat{\mu}}{\partial^2 m} \leq 0.$$

Due to the symmetry in  $o$  and  $m$ , it is enough to verify  $\frac{\partial^2 \hat{\mu}}{\partial^2 m} \leq 0$  and  $\frac{\partial^2 \hat{\mu}}{\partial o \partial m} \leq 0$ .

$$\frac{\partial \hat{\mu}^2}{\partial o \partial m} = -\frac{\hat{C}^{\hat{\alpha}_1 \hat{\alpha}_2} (t_0 - \hat{C}(o+1)^{\hat{\alpha}_2} (m+1)^{\hat{\alpha}_1}) (m+1)^{\hat{\alpha}_1-1} (o+1)^{\hat{\alpha}_2-1}}{(t_0 + \hat{C}(m+1)^{\hat{\alpha}_1} (o+1)^{\hat{\alpha}_2})^3}, \quad (\text{EC.9})$$

$$\frac{\partial \hat{\mu}^2}{\partial^2 o} = -\frac{\hat{C}^{\hat{\alpha}_2} (t_0(\hat{\alpha}_2 - 1) - \hat{C}(1 + \hat{\alpha}_2)(m+1)^{\hat{\alpha}_1} (o+1)^{\hat{\alpha}_2}) (m+1)^{\hat{\alpha}_1} (o+1)^{\hat{\alpha}_2-2}}{(t_0 + c(m+1)^{\hat{\alpha}_1} (o+1)^{\hat{\alpha}_2})^3}. \quad (\text{EC.10})$$

Since  $\hat{\alpha}_1 < 0$ ,  $\hat{\alpha}_2 < 0$ , and  $t_0 - \hat{C}(o+1)^{\hat{\alpha}_2}(m+1)^{\hat{\alpha}_1} \geq t_0 - \hat{C} \geq 0$ , it follows from equation (EC.9) that  $\frac{\partial \hat{\mu}^2}{\partial o \partial m} \leq 0$ . Next, for the second derivative with respect to  $o$ , we use the fact that  $\hat{\alpha}_2 < 0$  and we have:

$$\begin{aligned} & t_0(\hat{\alpha}_2 - 1) - \hat{C}(1 + \hat{\alpha}_2)(m+1)^{\hat{\alpha}_1}(o+1)^{\hat{\alpha}_2} \\ &= -t_0 - \hat{C}(m+1)^{\hat{\alpha}_1}(o+1)^{\hat{\alpha}_2} + \hat{\alpha}_2 \left( t_0 - \hat{C}(m+1)^{\hat{\alpha}_1}(o+1)^{\hat{\alpha}_2} \right) \\ &\leq \hat{\alpha}_2 \left( t_0 - \hat{C}(m+1)^{\hat{\alpha}_1}(o+1)^{\hat{\alpha}_2} \right) \\ &\leq 0, \end{aligned}$$

which implies that  $\frac{\partial \hat{\mu}^2}{\partial o^2} \leq 0$  from equation (EC.10). This completes the proof.  $\square$